

# Blind Walking of a Planar Biped on Sloped Terrain

by

Chee-Meng Chew

B.Eng. Mech. (Hons)  
National University of Singapore

SUBMITTED TO THE DEPARTMENT OF MECHANICAL ENGINEERING  
IN PARTIAL FULFILLMENT OF THE REQUIREMENTS FOR THE DEGREE OF

MASTER OF SCIENCE IN MECHANICAL ENGINEERING  
AT THE  
MASSACHUSETTS INSTITUTE OF TECHNOLOGY

FEBRUARY 1998

© 1998 Chee-Meng Chew. All rights reserved.

The author hereby grants to MIT permission to reproduce  
and to distribute publicly paper and electronic  
copies of this thesis document in whole or in part.

Signature of Author .....

Department of Mechanical Engineering

January 16, 1998

Certified by .....

Gill A. Pratt

Assistant Professor, Electrical Engineering and Computer Science

Thesis Supervisor

Certified by .....

Jean-Jacques E. Slotine

Professor, Mechanical Engineering

Thesis Reader

Certified by .....

Ain A. Sonin

Chairman, Departmental Committee on Graduate Students

APR 27 1998

LIBRARIAN

# Blind Walking of a Planar Biped on Sloped Terrain

by

Chee-Meng Chew

Submitted to the Department of Mechanical Engineering  
on January 15, 1998 in Partial Fulfillment of the  
Requirements for the Degree of Master of Science in  
Mechanical Engineering

## ABSTRACT

This thesis demonstrates the successful application of Virtual Model Control (VMC) to a simulated seven-link planar biped for walking *dynamically* and *steadily* over sloped terrain with unknown slope gradients and transition locations. The slope gradients were assumed to be between  $\pm 20^\circ$ ; and it had maximum transitional gradient change of less than  $20^\circ$  per step. The developed algorithm for sloped terrain walking was based on a level ground implementation with only minor changes. This thesis adopted the same virtual components, which included a vertical spring-damper, a horizontal damper and a rotational spring-damper, to generate the required torque at the joints. The biped used the natural compliance of swing foot so that it could land flat onto an unknown slope. After the complete touch down of the swing foot, a *global slope* was computed and this was used to define a *virtual surface*. The algorithm then computed the desired hip height based on the global slope which resulted in a desired straight line trajectory parallel to the virtual surface. The algorithm was very simple and did not require the biped to have an extensive sensory system for blind walking over slopes. The ground was detected only through foot contact switches. The knowledge required for the implementation mainly consisted of intuition and geometric considerations.

This thesis also demonstrates the replacement of the vertical virtual spring-damper with Robust Adaptive Controller and the successful implementation with the biped walking over random sloped terrain. This thesis also shows how the algorithm for sloped terrain walking can be extended to stair climbing.

Thesis Supervisor: Gill A. Pratt, Ph.D.

Title: Assistant Professor of Electrical Engineering and Computer Science

## Acknowledgments

---

I am indebted to all my lab mates for their contributions to my knowledge and awareness in my research area, especially Jerry Pratt and Dr. Robert Ringrose who never got tired of answering all my doubts and helping me when I ran into problems. I also thank Jerry for designing and building the planar biped “Spring Flamingo” which allowed me to set an application target for my research. I would also like to thank all the present and former lab members who contributed to the design of the simulation package, especially the Creature Library, without which my research would be very tedious. Thanks also to Peter Dilworth and Jerry for adding terrain features in the simulation package. I wish to thank my advisor, Prof. Gill A. Pratt, for letting me take on this research and giving me the freedom to undertake it. I also wish to thank Prof. Jean-Jacques Slotine for being the reader for this thesis in spite of his tight schedule. I would like to thank Jerry, Dave Robinson and Prof. Pratt for proof reading my thesis. My work at MIT would never have happened without the sponsorship of the National University of Singapore. I wish to thank my wife and daughter for being very understanding and for providing me with moral support just at the right moment. I am also very grateful to God, the Creator or Mother Nature for creating the physical world which is imbued with an uncountable number of intriguing phenomena and laws for us to explore.

# Contents

---

<b>1 INTRODUCTION.....</b>	<b>8</b>
1.1 BACKGROUND.....	8
1.2 PREVIOUS WORK .....	9
1.3 OBJECTIVE AND SCOPE.....	10
1.4 OUTLINE OF THE THESIS.....	10
<b>2 SEVEN-LINK PLANAR BIPED.....</b>	<b>12</b>
<b>3 VIRTUAL MODEL CONTROL.....</b>	<b>15</b>
3.1 TASK CHARACTERISTICS AND SPECIFICATIONS FOR STEADY DYNAMIC WALKING OF A BIPED.....	15
3.2 CONCEPT OF VIRTUAL MODEL CONTROL .....	16
3.3 APPLICATION TO STEADY DYNAMIC WALKING OF BIPED.....	17
3.3.1 <i>Walking control using the state machine</i> .....	19
3.3.2 <i>Swing leg strategy</i> .....	21
3.3.3 <i>Key parameters</i> .....	21
<b>4 ROBUST ADAPTIVE CONTROL .....</b>	<b>26</b>
4.1 BACKGROUND.....	26
4.2 THEORY .....	26
4.3 APPLICATION OF ROBUST ADAPTIVE CONTROL TO BIPED WALKING.....	28
4.4 SIMULATIONS RESULTS.....	30
4.4.1 <i>Effect of <math>\lambda</math></i> .....	30
4.4.2 <i>Effect of <math>k</math></i> .....	31
4.4.3 <i>Effect of <math>D</math></i> .....	32
4.4.4 <i>Effect of <math>\gamma</math></i> .....	32
4.4.5 <i>Effect of <math>\hat{m}_o</math></i> .....	32
4.5 DISCUSSION .....	36
4.6 CONCLUSION .....	36
<b>5 SLOPED TERRAIN WALKING .....</b>	<b>37</b>
5.1 SLOPED TERRAIN WALKING USING VIRTUAL MODEL CONTROL .....	38
5.1.1 <i>Upslope and downslope walking</i> .....	38
5.1.2 <i>Transition cases</i> .....	41
5.2 EXTENSION TO DYNAMIC STAIR-WALKING .....	46
<b>6 SIMULATIONS RESULTS.....</b>	<b>47</b>
6.1 SLOPED TERRAIN PROFILES USED IN THE SIMULATIONS .....	47
6.2 WALKING OVER THE SLOPED TERRAIN PROFILE ONE .....	48
6.3 WALKING OVER THE SLOPED TERRAIN PROFILE TWO.....	53
6.4 WALKING ON STAIRS .....	56
6.5 DISCUSSION .....	58
<b>7 CONCLUSIONS AND FURTHER WORK.....</b>	<b>60</b>
7.1 CONCLUSIONS.....	60
7.2 FURTHER WORK.....	60

**APPENDIX A: EQUATIONS TO CONVERT VIRTUAL FORCES TO JOINTS' TORQUE**

**APPENDIX B: STABILITY ANALYSIS BASED ON "MASSLESS LEGS" MODEL**

# List of Figures

---

FIGURE 1. BIPED ROBOT: “SPRING FLAMINGO” .....	12
FIGURE 2. SEVEN-LINK PLANAR BIPED MODEL .....	13
FIGURE 3. VIRTUAL MODEL CONTROL APPLYING TO TWO-LINK MANIPULATOR (POSITION CONTROL).....	17
FIGURE 4. VIRTUAL COMPONENTS USED FOR BIPED WALKING .....	18
FIGURE 5. STATE DIAGRAM FOR WALKING CONTROL.....	20
FIGURE 6. GEOMETRIC CONSTRAINT FOR CALCULATING $Z_{LIMIT}$ .....	23
FIGURE 7. MASSLESS LEG MODEL FOR THE BIPED .....	29
FIGURE 8. ROBUST ADAPTIVE CONTROL APPLIED TO Z-DIRECTION .....	30
FIGURE 9. ROBUST ADAPTIVE CONTROL: $\lambda = 0.2, \kappa = 50, \gamma = 10, D = 5, \hat{m}_o = 9$ .....	33
FIGURE 10. ROBUST ADAPTIVE CONTROL: $\lambda = 2, \kappa = 50, \gamma = 10, D = 5, \hat{m}_o = 9$ .....	33
FIGURE 11. ROBUST ADAPTIVE CONTROL: $\lambda = 5, \kappa = 50, \gamma = 10, D = 5, \hat{m}_o = 9$ .....	34
FIGURE 12. ROBUST ADAPTIVE CONTROL: $\lambda = 10, \kappa = 50, \gamma = 10, D = 5, \hat{m}_o = 9$ .....	34
FIGURE 13. ROBUST ADAPTIVE CONTROL: $\kappa = 100, \lambda = 2, \gamma = 10, D = 5, \hat{m}_o = 9$ .....	34
FIGURE 14. ROBUST ADAPTIVE CONTROL: $\kappa = 500, \lambda = 2, \gamma = 10, D = 5, \hat{m}_o = 9$ .....	34
FIGURE 15. ROBUST ADAPTIVE CONTROL: $D = 0.01, \lambda = 2, \kappa = 50, \gamma = 10, \hat{m}_o = 9$ .....	35
FIGURE 16. ROBUST ADAPTIVE CONTROL: $D = 20, \lambda = 2, \kappa = 50, \gamma = 10, \hat{m}_o = 9$ .....	35
FIGURE 17. ROBUST ADAPTIVE CONTROL: $\gamma = 50, \lambda = 2, \kappa = 50, D = 5, \hat{m}_o = 9$ .....	35
FIGURE 18. ROBUST ADAPTIVE CONTROL: $\hat{m}_o = 13, \lambda = 2, \kappa = 50, \gamma = 10, D = 5$ .....	35
FIGURE 19. FOUR TYPICAL GEOMETRIES OF TERRAIN: (A) A GRADIENT (B) A DITCH (C) A VERTICAL STEP (D) AN ISOLATED WALL [SONG AND WALDRON, 1989].....	37
FIGURE 20. GEOMETRIC CONSTRAINT TO CALCULATE $H_{LIMIT}$ : LEVEL AND UPSLOPE .....	40
FIGURE 21. GEOMETRIC CONSTRAINT TO CALCULATE $H_{LIMIT}$ DURING DOWNSLOPE WALKING: (A) CASE 1; (B) CASE 2 .....	41
FIGURE 22. NATURAL COMPLIANCE OF THE SWING FOOT .....	42
FIGURE 23. (A) GLOBAL SLOPE WHOSE GRADIENT IS DIFFERENT FROM THAT OF THE ACTUAL SLOPE; AND (B) GLOBAL SLOPE WHOSE GRADIENT IS THE SAME AS THAT OF THE ACTUAL SLOPE. ....	44
FIGURE 24. EXTREME EXAMPLE TO DEMONSTRATE A POTENTIAL PROBLEM WHEN THE LOCAL SLOPE IS USED TO CALCULATE THE DESIRED HIP HEIGHT. ....	44
FIGURE 25. SEQUENCE FOR LEVEL-TO-DOWNSLOPE TRANSITION.....	45
FIGURE 26. POSSIBLE PROBLEM WITH SWING LEG .....	45
FIGURE 27. GLOBAL SLOPE IN STAIR-WALKING .....	46
FIGURE 28. STICK DIAGRAM OF THE BIPED WALKING OVER THE SLOPED TERRAIN <i>PROFILE ONE</i> FROM LEFT TO RIGHT (SPACED APPROXIMATELY 0.08 S APART AND SHOWING ONLY THE LEFT LEG).....	50
FIGURE 29. PROFILES OF THE KEY VARIABLES WHEN THE BIPED WALKED OVER THE SLOPED TERRAIN <i>PROFILE ONE</i> .....	51
FIGURE 30. TORQUE PROFILES OF THE HIP AND THE KNEE JOINTS WHEN THE BIPED WALKED OVER THE SLOPED TERRAIN <i>PROFILE ONE</i> .....	52
FIGURE 31. PROFILES OF THE KEY VARIABLES WHEN THE BIPED WALKED OVER SLOPED TERRAIN <i>PROFILE TWO</i> .. .....	54
FIGURE 32. VARIABLES’ PROFILES OF THE BIPED WALKING OVER THE SLOPED TERRAIN <i>PROFILE TWO</i> USING ROBUST ADAPTIVE CONTROLLER AS THE VERTICAL VIRTUAL COMPONENT ( $\lambda = 2, \kappa = 100, \gamma = 10, D = 5,$ $\hat{m}_o = 9$ ).....	55
FIGURE 33. STICK DIAGRAM OF THE BIPED WALKING ON THE STAIRS (SPACED APPROXIMATELY 0.2 S APART AND SHOWING ONLY THE LEFT LEG) .....	56
FIGURE 34. OUTPUT VARIABLES PROFILES OF THE BIPED WALKING OVER THE STAIRS .....	57

# List of Tables

---

TABLE 1. INERTIA PARAMETERS OF THE SIMULATED BIPED .....	14
TABLE 2. LENGTH PARAMETERS OF THE SIMULATED BIPED.....	14
TABLE 3. DESCRIPTIONS OF THE STATES USED IN THE BIPED WALKING CONTROL .....	20
TABLE 4. GAITS' PARAMETERS.....	21
TABLE 5. PARAMETERS OF VIRTUAL COMPONENTS.....	21
TABLE 6. DESIRED VALUES OF SOME OF THE GAITS' VARIABLES AND THE PARAMETERS OF THE VIRTUAL COMPONENTS SET IN THE SIMULATION .....	48

# Chapter

## 1 Introduction

---

### 1.1 Background

Biped locomotion is a hot area in legged locomotion research. One reason is that humans are themselves bipedal creatures and we hope to gain better insight into how human beings walk and run. Another reason is that bipeds provide a great control challenge for engineers and scientists. Compared with robots that have more than two legs, bipeds usually have a lesser number of actuators, and hence they are lighter in weight and lower in cost. They also require a smaller foothold area for locomotion and thus are more versatile.

The task of controlling a biped to walk *statically* is easy but the resulting motion is slow. However, a control algorithm for it to walk *dynamically* is usually complex and requires heavy computation. Past researchers have tried to model biped locomotion using methods like Lagrangian or Newton-Euler mechanics. The resulting dynamic equations for the models were usually of high order and needed to be simplified by some assumptions before a control technique could be applied. For example, [Furusho and Masubuchi, 1986] derived the full equations of motion for a five-link planar biped and then linearized them around the vertical equilibrium and partitioned the linearized state equations into dominant and fast modes. The dynamics of the fast modes were ignored and proportional plus derivative feedbacks were applied at individual joints to track prescribed angular displacement profiles. The trajectory tracking was carried out in the joint space. [Kajita and Tani, 1991] studied a planar biped which was modelled as a massive body with two massless legs. The biped was controlled to walk in a mode called “Linear Inverted Pendulum”.

A control methodology called “Virtual Model Control” (VMC) [Pratt, 1995] was recently developed for legged robots. This method is based on intuition. The resulting controller does not need the dynamics information in order for a legged robot to perform *steady*<sup>1</sup> dynamic walking. Thus, it allows a computationally less intense framework for the control since it does not require the computation of inverse dynamics for the legged robot. [Pratt, 1995] has successfully used the VMC to control a planar biped to walk on flat ground.

---

<sup>1</sup> Meaning the average horizontal velocity is constant.



Most research on biped locomotion has been restricted to level ground locomotion. Few have implemented bipeds that could walk on rough terrain. Without the capability of adapting to rough terrain, any legged machine will defeat the purpose of its existence since the ability to adapt to rough terrain is one of the most important reasons for legged locomotion. This provides us with a very good motivation to extend the VMC to rough terrain locomotion of a biped.

## 1.2 Previous work

[Zheng and Shen, 1990] have done research on a biped (SD-2) which walked on a slope in a *statically* stable way. The biped had force sensors at the feet to detect the transition of the supporting terrain from a flat floor to a slope and used a compliant motion scheme to adapt the landing foot to an unknown terrain. Joint positions were then used to calculate the inclination of the landing foot as well as the slope gradient. They found that the slope walking of the biped involved simple modifications to a level walking gait. They simply modified the torso's pitching angle so that the center of gravity of the biped was shifted to the most stable<sup>2</sup> position. They also developed a transitional walking gait for SD-2 to walk from level ground to a slope, and vice versa. The same walking gait could be used for walking on level ground or on a slope. The implementation of the strategy was simple. However, it was only applied to static walking which had a slow locomotion speed.

[Yamaguchi, et al., 1996] introduced an anthropomorphic *dynamic* biped walking robot (WL-12RVII) which could adapt to a humans' living floor. The biped had a special foot system (WAF-3) which was used to obtain a position relative to a landing surface and the gradient of the surface during its dynamic walking. The biped used an "adaptive walking control system" to adapt to path surfaces with unknown shapes by utilizing information concerning the landing surface obtained by the foot system. The biped was able to perform dynamic walking and yet adapt to a humans' living floor with an unknown shape. The maximum walking speed was 1.28 s/step with a 0.3 m step length, and the adaptable deviation range was from -16 to +16 mm/step in the vertical direction, and from -3° to +3° for the tilt angle. These capabilities of the biped could be attributed mainly to the extensive design of the feet.

[Kajita and Tani, 1995] used a scheme called "Linear Inverted Pendulum Mode" to control a biped walking on rough terrain. They developed a simple control method for the biped by ignoring the mass of the legs. They assumed that the biped knew the profile of the ground in advance. Based on the predetermined foothold position for each step, a constraint line was calculated. The biped tried to follow the constraint line while keeping its body upright.

---

<sup>2</sup> In the static sense.

### 1.3 Objective and Scope

The objective of this thesis is to study the feasibility of applying the VMC to a planar<sup>3</sup> biped so that it can walk over slopes dynamically without knowing the gradients and the transition positions in advance. We wish to achieve the task by using the signals from two discrete ground contact sensors located at the bottom of the biped's feet. We also wish to achieve this task by *simple* modifications to the algorithm for level ground walking [Pratt, 1995]. The thesis will verify the modified algorithm by simulating a planar seven-link biped walking over sloped terrain.

The followings are the assumptions made in all the simulations:

1. It is assumed that the friction will be high enough to prevent any slippage once the feet touch the ground.
2. It is assumed that the biped has perfect actuators which provide desired torque at each joint. In real systems, "Series Elastics Actuators" [Pratt and Williamson, 1995] are used to provide the desired torque at each joint.
3. The sloped terrain does not have step variations and the transition location between two different slope gradients is smooth. There is also no variation of terrain in the transverse direction.

### 1.4 Outline of the thesis

*Chapter 2* describes the configuration and parameters of the biped simulation model used in this thesis. The model is based on a physical planar seven-link biped called "Spring Flamingo".

*Chapter 3* describes the basic idea of Virtual Model Control and its application to the biped. It then gives qualitative descriptions of the key parameters for walking control of the biped.

To maintain a nominal height of the biped when there is a change in the load applied onto it, *Robust Adaptive Controller* [Slotine and Coetsee, 1986] is introduced into the control algorithm in *Chapter 4*. Several simulation results are included for the study of the effect of Robust Adaptive Control's parameters.

*Chapter 5* includes a strategy developed for the sloped terrain walking of the biped. This strategy allows the biped to walk blindly over a series of slopes. It also explains how the same strategy can be extended to stair climbing.

---

<sup>3</sup> Constrained to move in sagittal plane only.

*Chapter 6* includes all the simulation results of the sloped terrain walking of the biped. It also includes stair climbing simulation results. These results are used to validate the strategy developed in Chapter 5. A general discussion is included at the end of this chapter.

*Chapter 7* includes the conclusions and the future work that can be extended from this thesis.

# Chapter

## 2 Seven-link Planar Biped

---

In most control problems, the control methods adopted usually depend on the particular design of the plant. This is also true for biped locomotion. The control strategies studied in this thesis are designated for a physical six-d.o.f. seven-link planar biped called “Spring Flamingo” (see Figure 1) which was designed and built recently by Jerry Pratt in the *Leg Laboratory*<sup>4</sup>. It has two slim legs and a torso. Each leg consists of a hip joint, a knee joint and an ankle joint. All the joints are revolute pin joints with axes perpendicular to the sagittal plane.

Each joint has a rotary potentiometer attached to measure the relative angles between two adjacent links. The relative angular velocity is obtained by an analog differentiator mounted on board the biped. The pitch angle of the biped’s torso is measured by a rotary potentiometer attached between the boom<sup>5</sup> and the torso. Each foot has two discrete sensors, one of which is positioned at the toe and the other at the heel. The sensors’ outputs are used to determine whether the biped’s foot is fully touched down, heel down only, toe down only, or foot in the air.

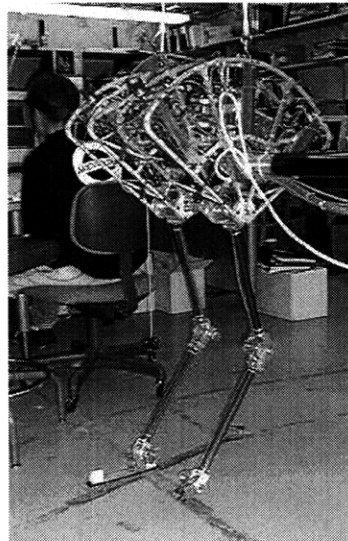


Figure 1. Biped robot: “Spring Flamingo”

---

<sup>4</sup> One of the research group belonging to the AI lab of MIT.

<sup>5</sup> This is used to constrain the biped to walk in a circle.

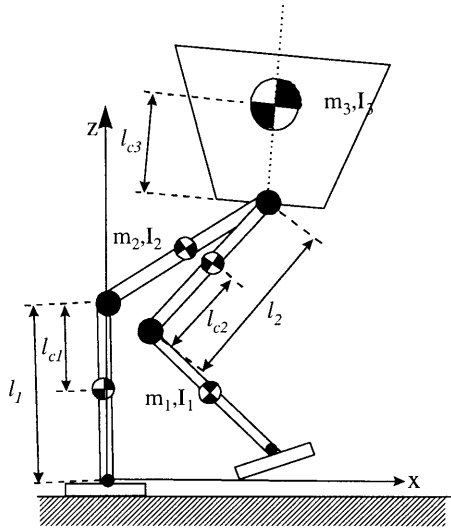


Figure 2. Seven-link planar biped model

If we assume that during the single support phase, the ankle of the swing leg is fixed and there is no actuation at the ankle of the stance leg, the dynamic equations for the biped during the single support phase is similar to those derived in [Furusho and Masubuchi, 1986] for a five-link planar biped.

An equivalent computer model (as shown in Figure 2) was created and it has approximately the same configuration and mass distribution as *Spring Flamingo*. The parameters of this model are tabulated in Table 1 and Table 2.

The simulation environment mainly consists of a dynamics simulator package (SD-FAST<sup>6</sup>) and a proprietary software library. The proprietary software library was written by past and present affiliates of Leg Lab. It includes functions for model creation (Creature Library), ground contacts specifications, terrain specifications, etc.. After setting up the computer model for the biped, the user is required to design a control algorithm in C code. The control function is called every “*control\_dt*” seconds to supply the desired torque or forces to the model’s actuators.

---

<sup>6</sup> Product of Symbolic Dynamics.

Table 1. Inertia parameters of the simulated biped

Part	Mass (kg)	Moment of inertia about the center of mass, $I_{yy}$ (kg m <sup>2</sup> )
Torso	10.0	$3.41 \times 10^{-2}$
Upper leg link	0.460	$1.30 \times 10^{-4}$
Lower leg link	0.306	$5.70 \times 10^{-5}$
Foot	0.251	$3.70 \times 10^{-4}$
Total mass	12.03	

Table 2. Length parameters of the simulated biped

Description	Value
<i>Torso</i>	
Height of center of mass referred from hip, $l_{c3}$	0.2 m
<i>Upper leg link</i>	
Length of upper leg link, $l_2$	0.42 m
Distance of center of mass of the upper leg from the knee joint, $l_{c2}$	0.117 m
<i>Lower leg link</i>	
Length of lower leg link, $l_1$	0.42 m
Distance of center of mass of the lower leg from the ankle joint, $l_{c1}$	0.238 m
<i>Foot (Symmetrical)</i>	
Foot length	0.15 m
Distance from ankle joints to foot based	0.04 m

# Chapter

## 3 Virtual Model Control

---

In biped locomotion, it is generally difficult to transform from high level task specifications, such as “walk forward” to low level motion control such as the required joint torques or trajectories. Furthermore, the dynamic equations of a biped are usually of high order. Even if we can derive the dynamic equations for the biped, we still face the problem of underactuation at the ankle during single support.

In the implementation of biped walking, one common approach is to compute and command the joint space trajectories at each phase of the walking gait and this is mostly based on a desired trajectory (e.g. of the body) in the cartesian space or some pattern generators, etc.. The desired joints’ trajectories can be achieved by nonlinear control techniques like *computed torque control* [Mitobe et al., 1995], *robust control* [Tzafestas et al., 1996], *adaptive control* [Yang, 1994], etc.. However, this way of controlling a biped is computationally intensive as we need to compute the inverse dynamics. To avoid such complexity, some researchers linearize the nonlinear dynamic equations of the biped and apply *modern control techniques*.

The *Leg Laboratory* has developed a new control approach called *Virtual Model Control (VMC)* for the implementation of legged locomotion. The framework of this approach was well defined in [Pratt, 1995] and a comparison with other techniques like *Impedance Control*, *Stiffness Control* etc. was also included. This chapter gives a brief introduction to this approach and elaborates the details used by the biped to perform steady dynamic walking on *level* terrain. It will also provide a qualitative description of the control parameters. This approach will be extended to sloped terrain walking in Chapter 5.

### 3.1 Task characteristics and specifications for steady dynamic walking of a biped

Before we decide on the control approach to a system, it is important to first examine the desired task for the system. This thesis assumes that the task goal for the biped described in Chapter 2 is to realize a steady dynamic walking gait in the sagittal plane, while maintaining an upright posture for the torso. It also assumes that the walking gait consists of two main phases: single support and double support. Note that when the biped is in the single support phase, it is inherently unstable (just like an inverted pendulum) due to the gravity force. Thus, it is not possible to track any arbitrary trajectory as in a manipulator arm even if it is within the non-singular workspace. The stability of the biped is maintained by alternating between the left and right support phases in the right cycle.

One characteristic of *natural* biped walking is that the exact trajectory of the torso is not important. For example, in human walking, we usually do not specify a walking task by numbers. We simply try to maintain a generally upright position and interact with gravity and ground friction to perform stable walking. The specification for the horizontal walking velocity is always fuzzy. For example, we think in terms of “fast”, “medium”, “slow” motion etc.. It has been shown that a planar biped can walk passively down a gentle slope without any actuators [McGeer, 1990].

In this thesis, we specify the desired height and velocity of the torso, while keeping it in an upright position. However, the height and horizontal velocity are allowed to vary within a tolerable range. So, the next question is whether we need a very complex and precise dynamic model for the biped to achieve such specifications. The next section describes a simple method called Virtual Model Control which has been successfully implemented on a five-link planar biped permitting it to walk steadily on level ground.

### 3.2 Concept of Virtual Model Control

In Virtual Model Control (VMC) [Pratt, 1995], we use virtual components (e.g. springs, dampers etc.) to generate the required actuators’ forces. By attaching virtual components (which usually have corresponding physical parts, for example, a spring and a damper) at some locations of the biped, the biped will behave dynamically as if the actual physical components are attached to it provided that the actuators are perfect<sup>7</sup>.

Virtual Model Control approach results in a control algorithm which examines the virtual components to obtain virtual forces from their constitutive equations. Then these forces can be transformed to the actuator space by a transformation matrix. By changing the set points of the virtual components, we create an inequilibrium to the system; it will then adjust itself so that a new equilibrium position is reached.

The main mathematical data used in this approach is the Jacobian transformation matrix which relates the force vector in one space to another space. For example, in robotics application, we usually transform a force vector  $\vec{F}$  in the cartesian space to an equivalent torque vector  $\vec{\tau}$  in the joint space [Asada, 1986] by the following expression:

$$\vec{\tau} = {}^A_B J^T {}^A_B \vec{F} \quad (3.1)$$

---

<sup>7</sup> Meaning the actuators have infinite bandwidth. If the actuators have finite bandwidth, then the resulting performance will still be reasonable if the desired motion stays within the bandwidth.



where  ${}^A_B J$  is the Jacobian matrix which transforms the differential variation in the joint space into the differential variation of  $B$  frame with respect to  $A$  frame in the cartesian space. In Virtual Model Control,  $B$  and  $A$  frames correspond to the action frame and reaction frame, respectively [Pratt, 1995].

Equation (3.1) requires much lower computation compared to inverse kinematics and dynamics. This transformation is also well-behaved since, for a given force vector in the cartesian space, we can always obtain a corresponding torque vector in the joint space even if the robot is in a singular configuration.

The idea of the VMC can be illustrated using a planar two-linked manipulator as shown in Figure 3. We attach two fictitious or virtual spring-dampers to the end point of the manipulator. Based on intuition, we know that if the virtual spring-dampers have properties similar to their physical counterparts, the end position of the manipulator will settle at an equilibrium position. At the equilibrium position, the actual end-point effect of the joint torques is equal to the virtual forces of the virtual components. This is also similar to the application of the Proportional and Derivative control of the manipulator in the joint space. By shifting the set point of the virtual components, we can cause the end point of the manipulator to move to a new equilibrium position. Note that the manipulator will behave dynamically in the same way as if the manipulator had zero joints' torque and a corresponding set of real spring-dampers<sup>8</sup> were attached at the tip. This concept is very important as it allows intuition to be applied in the VMC.

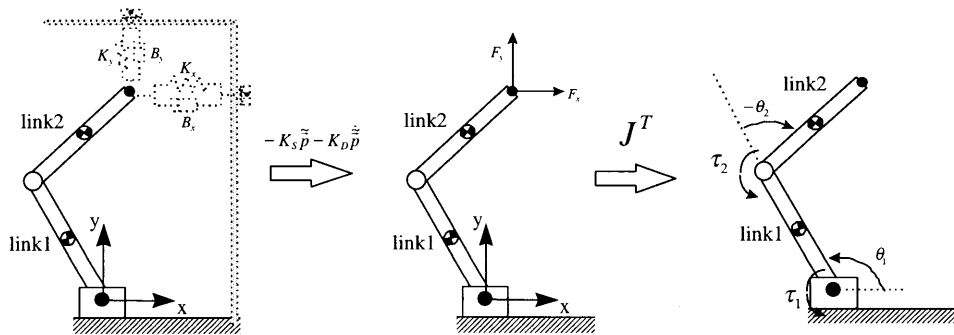


Figure 3. Virtual Model Control applying to two-link manipulator (Position control)

### 3.3 Application to steady dynamic walking of biped

In the implementation of biped walking using the VMC, the placements of virtual components require intuition; there may be more than one set of virtual components to achieve the global task defined in

<sup>8</sup> Those which have the same constitutive properties as the virtual components.

Section 3.1. Since we are interested in the motion described in cartesian space, it is natural for us to attach virtual components along each of the orthogonal coordinates in this space. One possible set of virtual components (same as those used by [Pratt, 1995]) is shown in Figure 4. A virtual spring-damper is attached to the hip along the vertical direction to generate a virtual vertical force  $F_z$  at the hip. It is used to control the vertical height of the biped. A virtual damper is attached to the hip along the horizontal direction to generate a virtual horizontal force  $F_x$  at the hip. This is used to control the horizontal velocity of the biped. A rotational spring-damper is attached at the hip to generate a virtual rotational force  $M_\alpha$  about the hip. This is used to maintain the upright posture of the biped's torso. The legs of the biped are bent towards the back during walking. That is, the biped walking bears more resemblance to birds than to humans.

Though the biped has actuated ankles, we set the ankle of stance leg to be limp by commanding a zero torque. This results in a motion similar to that of the previous 5-link biped [Pratt, 1995] which had no feet. The feet of the 7-link biped simply provide better traction during the single support phase. The usage of the ankle of the stance leg to modify the walking gait is beyond the scope of the thesis, but it has been implemented in the Leg Laboratory by Jerry Pratt.

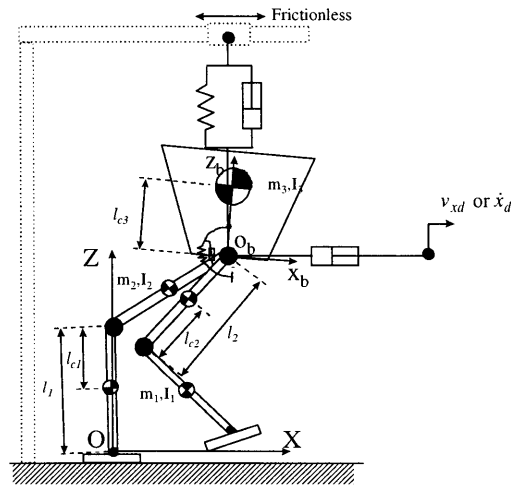


Figure 4. Virtual components used for biped walking

For our biped walking control, the inputs are the desired horizontal velocity  $\dot{x}_d$  (or  $v_{xd}$ ), the desired vertical height of the hip  $z_d$  and the desired pitch angle of the body  $\alpha_d$ . All these inputs define the desired motion of the body frame  $O_bX_bZ_b$  with respect to the inertia frame  $OXZ$ . Assuming the virtual components are linear, we can obtain the following control law in the cartesian frame:

$$F_x := b_x(\dot{x}_d - \dot{x}) \quad (3.2)$$

$$F_z := k_z(z_d - z) + b_z(\dot{z}_d - \dot{z}) \quad (3.3)$$

$$M_\alpha := k_\alpha(\alpha_d - \alpha) + b_\alpha(\dot{\alpha}_d - \dot{\alpha}) \quad (3.4)$$

where  $b_i$  and  $k_i$  are the damping coefficient and the spring stiffness, respectively for the virtual components in  $i$  ( $= x, z$  or  $\alpha$ ) coordinate.

However, this set of virtual components can only be applied to the double support phase and not to the single support phase. During the single support phase, since we have set the ankle of the stance leg to be limp, the biped loses one actuated degree of freedom. Thus, one of the virtual components cannot be realised. We chose to maintain the vertical and rotational spring-dampers and let the interaction between gravity and these virtual components dictate the horizontal velocity during this phase.

The virtual forces for both the single and the double support phases are transformed into the joint space using the equations derived in [Pratt, 1995]. A list of the equations can be found in Appendix A. Realtime control of the biped locomotion can be implemented based on a state machine and the equations. In this way, the VMC enables the biped to walk without computing the inverse dynamics and kinematics and hence simplifies the computation significantly.

### 3.3.1 Walking control using the state machine

The pattern of events, states, and state transitions of the biped walking can be represented by a *state diagram* (Figure 5). The states listed in Table 3 are used to identify distinct phases of control in a walking cycle. A software finite state machine is used to synchronise the state transitions by monitoring for some specified conditions in the sensory data. Note that such implementation provides organised handling of the sensory data, but it does not provide a foolproof solution unless we include all the possible discrete states in the algorithm.

Table 3. Descriptions of the states used in the biped walking control

State	Description
1. Double Support 1	Both feet are on the ground. Right foot is in front.
2. Right Support	The right foot is the stance leg and the left foot is the swing leg. Neither switch of the left foot is activated. The distance between the swing leg and the stance leg is less than the step length.
3. Single-to-Double Transition 1	This is the intermediate phase where Right Support state transits to Double Support 2.
4. Double Support 2	Both feet are on the ground. Left foot is in front.
5. Left Support	The left foot is the stance leg and the right foot is the swing leg. Neither switch of the right foot is activated. The distance between the swing leg and the stance leg is less than the step length.
6. Single-to-Double Transition 2	This is the intermediate phase where Left Support state transits to Double Support 1.

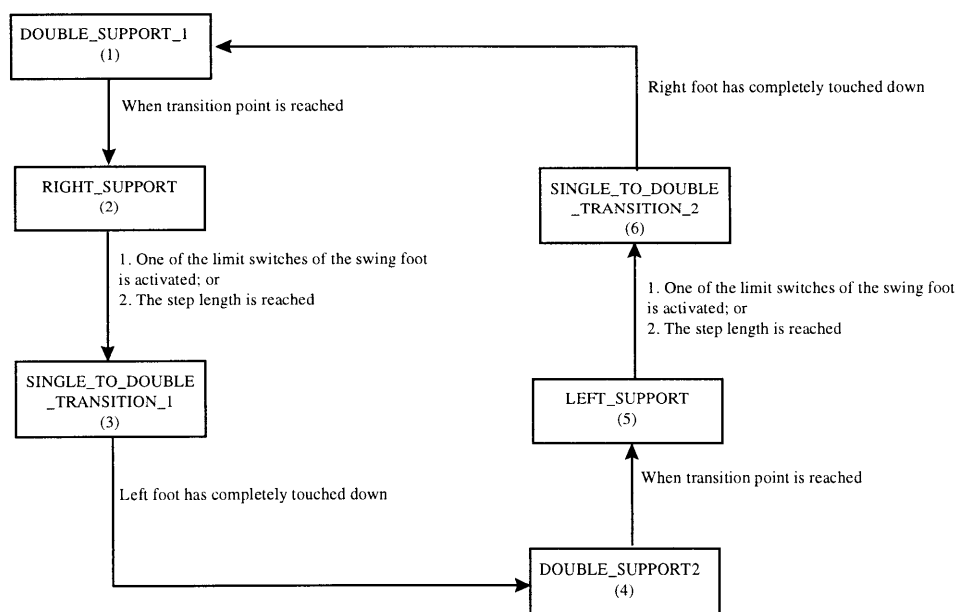


Figure 5. State diagram for walking control

### 3.3.2 Swing leg strategy

In the steady walking control considered in this thesis, the objective of a swing leg strategy is to achieve approximately the desired step length. When the swing leg touches down, we also want the vertical projection of the hip to be approximately at the center between the feet. The two key variables of the swing leg task are the desired step length  $s_l$  and the desired lift height  $h_l$ . These two variables will be discussed in the next subsection. The detailed control strategy for the swing leg is beyond the scope of this thesis.

### 3.3.3 Key parameters

This section highlights the key parameters that may affect the walking pattern and performance of the planar biped. They are mainly divided into gaits' (Table 4) and virtual components' (Table 5) parameters. This subsection provides a qualitative discussion of these parameters.

Table 4. Gaits' parameters

Parameter	Notation
Desired pitch angle of the torso	$\alpha_d$
Desired hip height	$z_d$
Desired horizontal velocity of the hip	$v_{xd}$
Desired step length	$s_l$
Distance from the front ankle at which double support phase transits to single support phase	$l_t$
Swing leg :	
a) Desired lift height	$h_l$
b) Swing time	$t_s$

Table 5. Parameters of virtual components

Parameter	Notation
1. Spring stiffness (in $z$ direction)	$k_z$
2. Damping coefficient (in $z$ direction)	$b_z$
3. Damping coefficient (in $x$ direction)	$b_x$
4. Spring stiffness (in $\alpha$ direction)	$k_\alpha$
5. Damping coefficient (in $\alpha$ direction)	$b_\alpha$

i) Desired pitch angle of the torso,  $\alpha_d$

This variable is used directly by the torsional virtual spring-damper. The simulated biped has a torso whose center of gravity is above the hip joints. By changing the maintained pitch angle of the torso, the projection of the overall biped's center of gravity can be shifted. When ascending a slope, the natural reaction for a human is to lean forward. When descending a slope, he naturally leans back as depicted by the photographs in [Muybridge, 1989]. However, to simplify matters, the desired pitch angle of the torso is set at zero degree in this thesis regardless of the slope gradient.

ii) Desired horizontal velocity at the hip,  $v_{xd}$

In biped walking, several approaches can be adopted to maintain the desired horizontal velocity. For example, we can control the horizontal velocity of a biped by foot placement [Raibert, 1986] as in the case of a hopping machine. In walking, we have a period where both feet are on the ground (double support) and this also can be utilised for horizontal velocity control.

In the previous analysis, we utilised a horizontal virtual damper to correct the horizontal velocity. Since the ankle torque is zero, the biped can only have this control (without sacrificing the vertical height and body pitch control) when it is in the double support phase. To prevent the divergence of the horizontal velocity, we want the double support duty cycle to be as large as possible. However, this approach to maintain the horizontal velocity may not be effective if the walking speed is high. This is because the actual duration of double support is very short during high speed walking. Also, although the equations developed in [Pratt, 1995] assumed that full horizontal force can be achieved during double support, this is not true in real applications since the foot of the biped is not hinged to the ground. Thus, we need to set a limit to the horizontal virtual force due to the virtual damper.

We can also modulate horizontal velocity by varying the transition position from double to single support. In single support, we want to have a swing leg control strategy that minimises the disturbance to the horizontal velocity.

iii) Desired hip height,  $z_d$

If the biped is in double support phase, the desired hip height is defined with respect to the ankle joint of the back supporting leg. Otherwise, it is defined with respect to the ankle joint of the stance leg. This variable is used by the vertical virtual spring-damper to compute the desired vertical force at the hip. At the singular configuration in which the stance leg or one of the legs during double support is fully

straightened, although the transformation equations do not “blow up”, the dynamics of the system is unpredictable. Thus, it is very important to select a proper hip height so that the leg of the biped will not reach the singular configuration. The upper limit is set by the geometry of the legs and the desired step length. This variable should not be too small since it will increase the required knee torque and hence the energy to maintain the biped’s height. This is due to the increase in the moment arm of the body weight with respect to the knee joints. Thus, we would like to have this variable close to the upper limit but not reaching it.

In the algorithm, the upper limit of the hip height  $z_{limit}$  was computed as in Equation (3.5):

$$z_{limit} = \sqrt{(l_1 + l_2)^2 - l^2} \quad (3.5)$$

where  $l = s_l + l_f$ ,  $s_l$  is the desired step length and  $l_f$  is the distance from the front ankle at which the double support phase transits to the single support phase.

We usually set the desired height at a fraction of this limit (using a factor  $k_{height}=0.8-0.9$ ) to cater to any discrepancy in the actual hip height and the actual step length. This will also allow the biped to better accommodate unknown terrain variations. Note that the foot’s dimension is ignored in the computation since we compute everything with respect to the cartesian frame attached to the ankle.

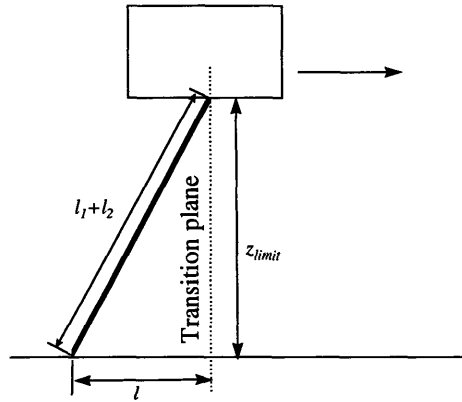


Figure 6. Geometric constraint for calculating  $z_{limit}$

iv) Desired step length,  $s_l$

This variable is used to plan the trajectory of the swing leg. It is coupled to the hip height as discussed before. We usually choose a desired step length depending on the lengths of the legs' links. In our present approach the double support phase is used mainly to correct the horizontal velocity. The step

length affects the relative period of the double support phase compared to the single support phase. Thus, this parameter indirectly affects the “controllability” of the horizontal speed of the locomotion.

v) Distance from the front ankle at which double support phase transits to single support phase,  $l$ ,

This is the projected horizontal distance of the hip from the ankle of the front leg where the biped changes from the double support phase to the single support phase. It should be forward enough so that the biped will not lose too much energy during the single support phase, otherwise it may lose all its forward momentum. It should not be forward to the extent that the forward velocity increases excessively after a single transition. The walking cycle may become unstable if the transition position is not properly selected.

vi) Lift height,  $h_l$  (For swing leg control)

This variable corresponds to the maximum lifting height of the swing leg during the swing motion and it is used in the trajectory planning of the swing leg. It may indirectly affect the degree of disturbance on the torso created by the swing leg. Its value is critical if the premature landing of the swing leg (e.g. in stair climbing) is undesirable.

vii) Swing time,  $t_s$  (For swing leg control)

This variable corresponds to the time available for the biped to swing its leg during the single support phase. This is calculated approximately from the velocity at the hip before the double to single support transition. As discussed in subsection 3.3.2, we want the hip of the torso to be roughly at the center, between the front and back supporting legs at touch down of the swing leg.

viii) Parameters of the virtual components

These parameters are tuned by trial and error. Some intuition based on the linear system helps too. For example, for the vertical virtual spring-damper, we would like to have sufficiently high spring stiffness for a sufficiently quick response. The damping coefficient is then adjusted so as to achieve overdamped response. The tuning process can be iterated if required. In actual implementation, the response of the virtual component is limited by the bandwidth of the actuators. Such an approach for tuning also applies to the rotational virtual spring-damper. Note that although the virtual spring-dampers are linear components, the resulting dynamic system is nonlinear. Hence, it is not desirable to have oscillatory motion in the resulting system as nonlinear oscillatory motion can be non-intuitive.



The tuning of the horizontal virtual damper is less stringent. It can be tuned after the other virtual components are done. As mentioned before, we have to set a limit to the virtual horizontal force generated by this virtual damper because the feet are not hinged onto the ground.

# Chapter

## 4 Robust Adaptive Control

---

### 4.1 Background

In the walking control of the planar biped, the previous chapter has demonstrated that a virtual spring-damper in the vertical direction can be used to control height. In the actual implementation, a constant offset term is added to compensate for the effective weight of the biped as perceived at the hip so that the biped can maintain close to the desired hip height without having a stiff virtual spring. However, it is not able to adapt to a varying torso mass which may occur if it carries an external load. For example, the biped will walk with a lower height if the torso's weight is increased. A possible solution would be to apply adaptive control in the joint space [Yang, 1994]. However, the inverse dynamics of a biped even in the planar case is very complex. This is complicated by the fact that in the single support phase, we lose an actuated degree of freedom at the ankle especially if the ankle is limp. Inspired by the VMC approach, this chapter will perform a feasibility study of the replacement of the existing vertical virtual component by *Robust Adaptive Controller* developed by [Slotine and Coetsee, 1986]. The purpose is to enable the biped to adapt to varying mass and walk with a height close to the desired value. The following sections will describe the theory of Robust Adaptive Control and how it can be applied to our biped to maintain its hip height.

### 4.2 Theory

This section includes the basic theory of Robust Adaptive Control. Since we are interested in a dynamics problem which is governed by the Newton's Second Law, let's consider the following second order nonlinear equation:

$$a_1\ddot{x} + a_2f(\dot{x}, x) + a_3g(x) + d(x, \dot{x}, t) = u \quad (4.1)$$

where  $a_1$ ,  $a_2$  and  $a_3$  are unknown constants,  $f(\dot{x}, x)$  and  $g(x)$  are nonlinear functions,  $d(x, \dot{x}, t)$  is the disturbance of known bound  $D$  (i.e.  $|d| \leq D$ ) and  $u$  is the input.

Definitions:

$$s(t) = \dot{\tilde{x}} + \lambda\tilde{x} = \dot{x} - \dot{x}_r, \quad (4.2)$$

where  $\tilde{z} = z - z_d$ ,  $\dot{\tilde{x}}_r = \dot{x}_d - \lambda \tilde{x}$  and  $\lambda$  is a strictly positive constant.

$$s_{\Delta}(t) = s(t) - \phi \text{sat}\left(\frac{s(t)}{\phi}\right) \quad (4.3)$$

The goal of the control is to make  $s_{\Delta} \equiv 0$  such that  $s$  is bounded by  $\phi$ . It can be shown that [Slotine and Li, 1991]

$$\forall t \geq 0, |s(t)| \leq \phi \Rightarrow \forall t \geq 0, |\tilde{x}^{(i)}(t)| \leq (2\lambda)^i \frac{\phi}{\lambda}, i=0,1. \quad (4.4)$$

To ensure that  $s_{\Delta}(\infty) \rightarrow 0$ , let's define

$$Y = [\tilde{x}_r \quad f(\dot{x}, x) \quad g(x)],$$

$$\bar{a} = [a_1 \quad a_2 \quad a_3]^T,$$

$$\tilde{a} = \hat{a} - \bar{a}.$$

where  $\hat{a}$  is the estimate of  $\bar{a}$ . We can choose the following Lyapunov candidate function

$$V = \frac{a_1}{2} s_{\Delta}^2 + \frac{1}{2} \tilde{a}^T \Gamma^{-1} \tilde{a}. \quad (4.5)$$

where  $\Gamma$  is a symmetric positive definite constant matrix. The time derivative of  $V$  is then given by

$$\begin{aligned} \dot{V} &= a_1 s_{\Delta} \dot{s} + \dot{\tilde{a}}^T \Gamma^{-1} \tilde{a} \\ &= s_{\Delta} (a_1 \ddot{x} - a_1 \ddot{x}_r) + \dot{\tilde{a}}^T \Gamma^{-1} \tilde{a} \\ &= s_{\Delta} (u - a_2 f - a_3 g - d - a_1 \ddot{x}_r) + \dot{\tilde{a}}^T \Gamma^{-1} \tilde{a} \end{aligned}$$

Let's define the control law as

$$u = Y \hat{a} - k s \quad (4.6)$$

where  $k$  is a strictly positive constant. Then

$$\dot{V} = s_{\Delta} Y \tilde{a} - s_{\Delta} d - k s_{\Delta} s + \dot{\tilde{a}}^T \Gamma^{-1} \tilde{a}.$$

By setting  $s_{\Delta} Y + \dot{\tilde{a}}^T \Gamma^{-1} = 0$ , we obtain the adaptation law

$$\dot{\tilde{a}} = -\Gamma Y^T s_{\Delta}. \quad (4.7)$$

Thus,  $\dot{V}$  becomes

$$\begin{aligned}\dot{V} &= -s_{\Delta}d - ks_{\Delta}(s_{\Delta} + \phi \text{sat}(\frac{s}{\phi})) \\ &= -s_{\Delta}d - ks_{\Delta}^2 - k|s_{\Delta}|\phi\end{aligned}$$

By setting  $k\phi = D$ , the resulting expression of  $\dot{V}$  is

$$\dot{V} \leq -ks_{\Delta}^2 \quad (4.8)$$

By Barbalat's Lemma [Slotine and Li, 1991], we can show that  $s_{\Delta} \rightarrow 0$  as  $t \rightarrow \infty$ .

### 4.3 Application of Robust Adaptive Control to biped walking

Based on the massless leg model as shown in Figure 7, we apply Robust Adaptive Control to the  $z$ -direction dynamic equation of the biped as shown below:

$$m\ddot{z} + mg + d(\bar{p}, \dot{\bar{p}}, t) = F_z \quad (4.9)$$

where  $m$  is the effective mass of the biped observed at the hip,  $\bar{p} = [x, z, \alpha]^T$  and  $d(\bar{p}, \dot{\bar{p}}, t)$  ( $|d| \leq D$ ) is the disturbance term which includes the variation<sup>9</sup> of the effective inertia and the effect of the swing leg dynamics. Note that the resulting system in the  $z$ -direction can be viewed to be a new "virtual component" for the VMC (Figure 8) which generates  $F_z$ , while the other two variables ( $v_{xd}$  and  $\alpha_d$ ) are still controlled using the virtual components described in Section 3.3.

Definitions:

$$\dot{z}_r = \dot{z}_d - \lambda \tilde{z}, \text{ where } \tilde{z} = z - z_d \quad (4.10)$$

$$s = \dot{\tilde{z}} + \lambda \tilde{z} = \dot{z} - \dot{z}_r \quad (4.11)$$

$$s_{\Delta} = s - \phi \text{sat}(\frac{s}{\phi}) \quad (4.12)$$

$$Ya = (\ddot{z}_r + g)m \quad (4.13)$$

where  $a = m$  and  $Y = (\ddot{z}_r + g)$

---

<sup>9</sup> Due to the variation in the effective weight of the legs as perceived at the hip.

The following control law (Equation (4.14)) and adaptation law (Equation (4.15)) are used:

$$F_z = Y\hat{a} - ks \quad (4.14)$$

$$\dot{\hat{a}} = -\gamma Y^T s_\Delta \quad (4.15)$$

where  $\gamma$  is a strictly positive scalar.

Note that, on level ground walking,  $\ddot{z}_d = 0$  and  $\dot{z}_d = 0$ . The following section study the effects of each variable ( $\lambda$ ,  $k$ ,  $\gamma$ ,  $D$ ,  $\hat{m}_o$ <sup>10</sup>) used by this Robust Adaptive Controller.

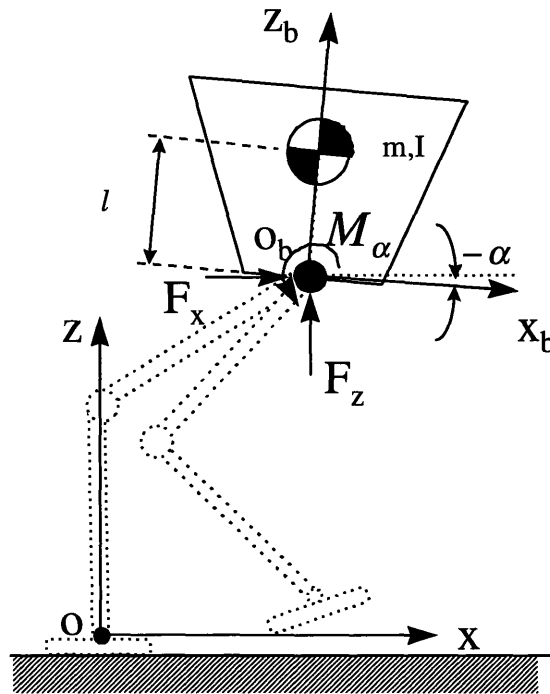


Figure 7. Massless leg model for the biped

<sup>10</sup> This variable is the initial estimate for  $m$ .

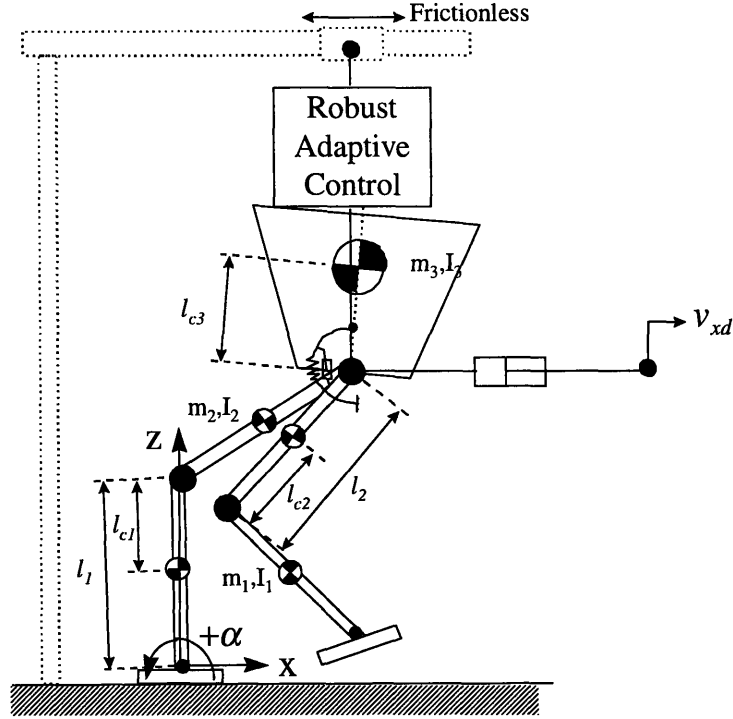


Figure 8. Robust Adaptive Control applied to  $z$ -direction

#### 4.4 Simulations results

In this section, the effects of the parameters ( $\lambda$ ,  $k$ ,  $\gamma$ ,  $D$ ,  $\hat{m}_o$ ) described in the previous section are studied based on level ground walking simulation of the biped. In all the simulations, the desired height of the hip was fixed at  $z_d=0.7$  m, the desired horizontal velocity was fixed at  $v_{xd}=0.4$  m/s and desired pitch angle was fixed at  $\alpha_d = 0$ . The initial conditions of the simulation were assigned to be the same as the desired value. The desired step length of the biped was fixed at 0.28 m.

##### 4.4.1 Effect of $\lambda$

We first varied  $\lambda$  while setting the other parameters as follows:  $k=50$ ,  $\gamma=10$ ,  $D=5$ ,  $\hat{m}_o=9$ . The simulation results for  $\lambda=0.2$ , 2, 5 and 10 are shown in Figure 9, Figure 10, Figure 11 and Figure 12, respectively.

Theoretically, when  $s_\Delta \rightarrow 0$ ,  $\tilde{z}$  will converge toward the bound  $(\phi/\lambda)$  (Equation (4.4)). Since  $\phi = D/k$  and both  $D$  and  $k$  were fixed in these simulations, large  $\lambda$  would result in small  $\tilde{z}$ . This is

demonstrated to be true by comparing the top graph of Figure 9, Figure 10, Figure 11 and Figure 12. Note that  $\lambda$  also behaves like the ratio of the proportional gain over the derivative gain in a PD controller. However, in a real system,  $\lambda$  is limited by the structural resonant modes, neglected time delays and sampling rate [Slotine and Li, 1991]. Furthermore, for biped locomotion, the foot is not fixed to the ground like that of a manipulator. So, we do not want  $\lambda$  to be too high.

From the top graph of Figure 9, we observed that when  $\lambda$  was too low, the bound ( $=\phi/\lambda$ ) for  $\tilde{z}$  became too big (Equation (4.4)) and the hip height fluctuated significantly. Due to the large fluctuation in the hip height, the biped's leg(s) reached singular configuration and resulted in instability.

It was observed that for all  $\lambda$ 's used here,  $\tilde{z}$  did not seem to converge to within the bound (given by  $\phi/\lambda$ ). This might be due to the fact that the disturbance bound  $D$  we set was too small compared to the real disturbances (e.g. due to the swing leg dynamics). That is, the results of the theoretical analysis we have done do not hold if selected  $D$  is smaller than the actual  $D$ . Interestingly, it was also observed that for  $\lambda=2$ ,  $\tilde{z}$  remained positive after the transient response had subsided.

Since we have mentioned that in our biped walking control, exact trajectory tracking is not important, the result of  $\lambda=2$  is acceptable and we set  $\lambda=2$  for the subsequent simulations. Besides, if  $\lambda$  is too high, it may cause the biped to be unstable if it walks on rough terrain.

#### 4.4.2 Effect of $k$

Equation (4.14) shows that the value of  $k$  influences the effect of  $s$  on  $F_z$ .  $k$  also directly affects  $\phi$  ( $=D/k$ ), which in turn affects the bound for  $\tilde{z}$  as discussed before. This subsection compares the simulation results of Figure 10, Figure 13 and Figure 14 to study the effect of  $k$ . The top graph of these figures verifies that as value of  $k$  increases, the bound for  $\tilde{z}$  becomes smaller. Large  $k$  also improved the transient response of  $\tilde{z}$  because it acts like a gain to the controller. However, when  $k$  was increased, the variation in the control input  $F_z$  was very high and abrupt (see the graph of  $F_z$  vs  $x$  in Figure 10, Figure 13 and Figure 14). Such variation in  $F_z$  may not be achievable in a real system if the required bandwidth is much larger than the actuator's bandwidth. Also, high  $k$  will retard the adaptation rate for  $\hat{m}$  (comparing the graph of  $\hat{m}$  vs  $x$  in Figure 10, Figure 13 and Figure 14) since the PD portion of the control law (Equation (4.14)) dominates in the contribution to the control input  $F_z$ .

### 4.4.3 Effect of $D$

The parameter  $D$  has direct influence on  $\phi$  ( $=D/k$ ). From the mathematical point of view, we want  $D$  to be small. However,  $D$  is determined by the actual disturbances. To study the effect of  $D$ , this subsection looks at the simulation results shown in Figure 10, Figure 15 and Figure 16.

Comparing the top graph of Figure 10 and Figure 16, the results demonstrated that when  $D$  was large, it indeed allowed a greater variation in  $\tilde{z}$ . Also, for the  $s_{\Delta}$  plot, we observed that the larger was  $D$ , the “quieter” was  $s_{\Delta}$  after the initial transient response.

For very small  $D$  as in Figure 15, we observed that  $\hat{m}$  was oscillatory. This was due to the adaptive controller trying to adapt to the disturbances. In contrast, the result in Figure 16 shows that  $\hat{m}$  converged smoothly to a constant value after some time.

### 4.4.4 Effect of $\gamma$

$\gamma$  appears in Equation (4.15) and hence it is one of the parameters which affects the adaptation rate for  $\hat{m}$ . It behaves like the gain of an *integral* controller. This subsection compares the simulation results between Figure 10 and Figure 17.

For higher  $\gamma$  (Figure 17), it was observed that  $\tilde{z}$  was smaller at the transient portion. This was because  $\hat{m}$  was being updated at a faster rate. However, after the transient portion of the response was over,  $\tilde{z}$  seemed to having the same behaviour and bound as shown in both figures. It was also observed that for high  $\gamma$ ,  $\hat{m}$  became rather oscillatory (comparing the graph of  $\hat{m}$  vs  $x$  in Figure 10 and Figure 17).

### 4.4.5 Effect of $\hat{m}_o$

This subsection studies the capability of the biped to adapt to step change (for example, due to loading and unloading of carried item) in effective mass. Instead of changing the effective mass (about 11 kg) of the biped, we changed  $\hat{m}_o$  (the initial value for  $\hat{m}$ ) so that it differed from the actual effective mass. When  $\hat{m}_o$  is smaller than actual effective mass (see Figure 10 where  $\hat{m}_o=9\text{kg}$ ), it corresponds to the instance when the biped just loads itself with an external load. When  $\hat{m}_o$  is greater than actual effective mass (see Figure 18 where  $\hat{m}_o=13\text{kg}$ ), it corresponds to the instance when the biped just unloads an external load. The simulation results showed that the biped indeed had the capability of adapting to the



changes in effective mass for both unloading and loading of an external load which was about 18% of the effective mass.

Note that the actual effective mass deviates from body mass (=10kg) because the former includes the effective mass of the leg(s) too. In the biped walking simulation, although we know the body mass, we do not have ready information about the effective mass of the leg. We need to obtain the inertial mass matrix referred to the hip and this is cumbersome. The properties of Robust Adaptive Control allows us to absorb part of the effective mass of the legs into  $\hat{m}$  and treat the rest of which as a disturbance.

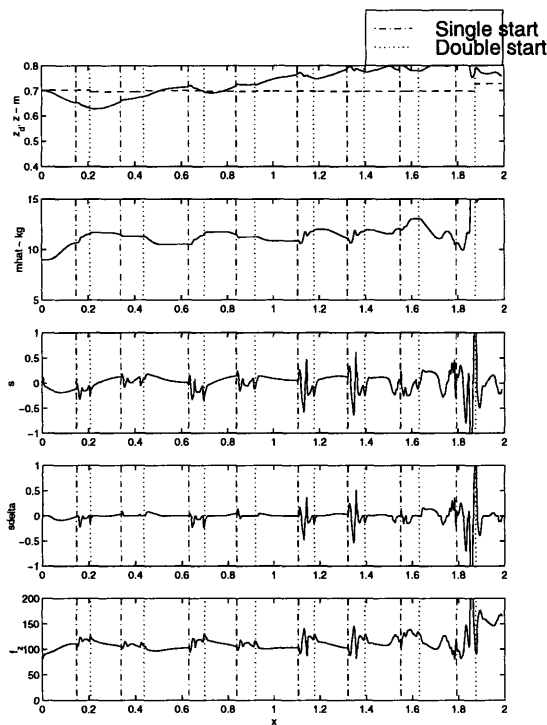


Figure 9. Robust Adaptive Control:  $\lambda = 0.2$ ,  $k=50$ ,  $\gamma = 10$ ,  $D=5$ ,  $\hat{m}_0 = 9$

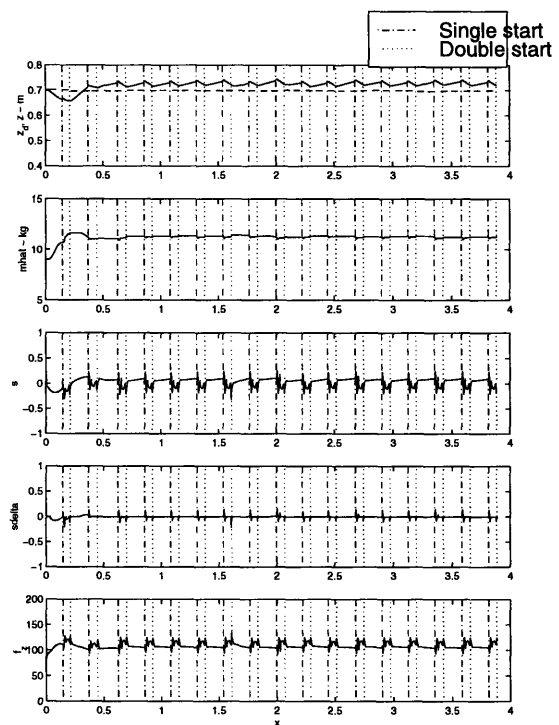


Figure 10. Robust Adaptive Control:  $\lambda = 2$ ,  $k=50$ ,  $\gamma = 10$ ,  $D=5$ ,  $\hat{m}_0 = 9$

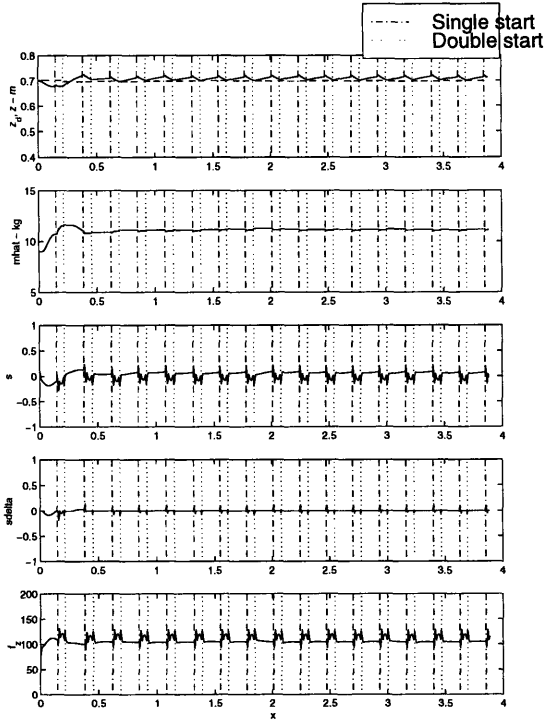


Figure 11. Robust Adaptive Control:  $\lambda = 5$ ,  $k=50$ ,  $\gamma = 10$ ,  $D=5$ ,  $\hat{m}_o = 9$

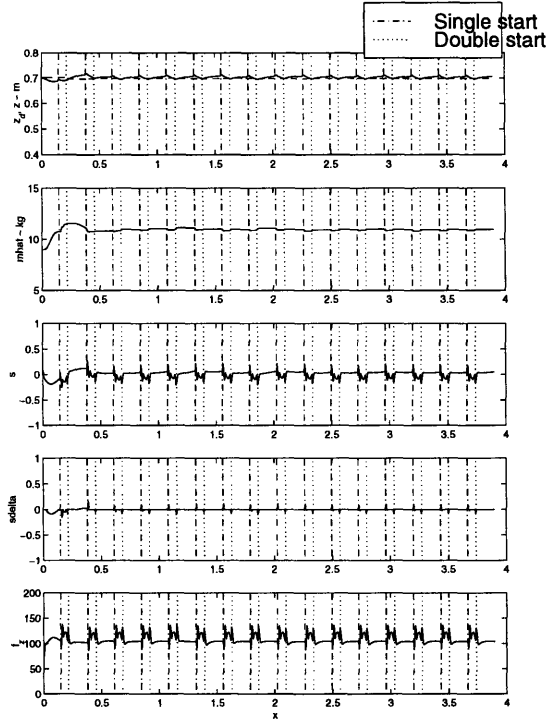


Figure 12. Robust Adaptive Control:  $\lambda = 10$ ,  $k=50$ ,  $\gamma = 10$ ,  $D=5$ ,  $\hat{m}_o = 9$

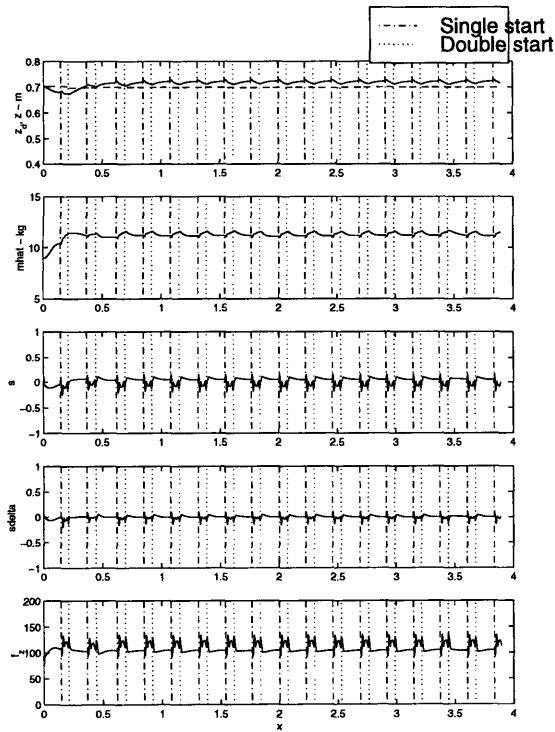


Figure 13. Robust Adaptive Control:  $k = 100$ ,  $\lambda = 2$ ,  $\gamma = 10$ ,  $D=5$ ,  $\hat{m}_o = 9$

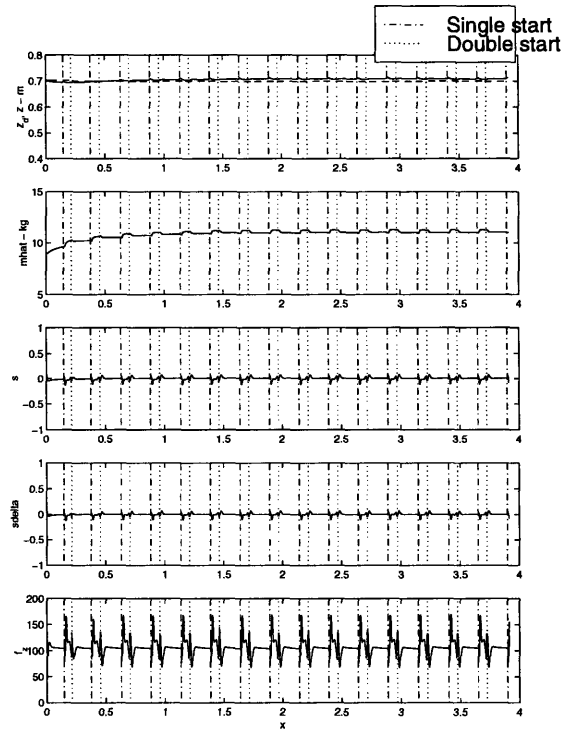


Figure 14. Robust Adaptive Control:  $k = 500$ ,  $\lambda = 2$ ,  $\gamma = 10$ ,  $D=5$ ,  $\hat{m}_o = 9$

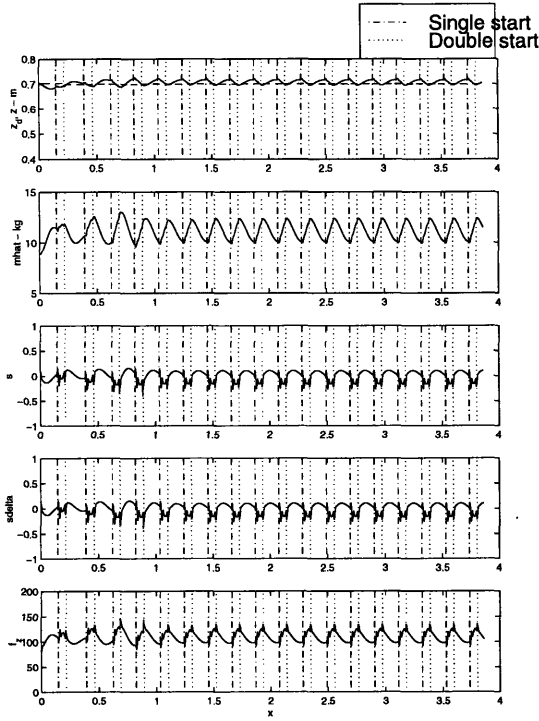


Figure 15. Robust Adaptive Control:  $D = 0.01$ ,  $\lambda = 2$ ,  $k=50$ ,  $\gamma = 10$ ,  $\hat{m}_o = 9$

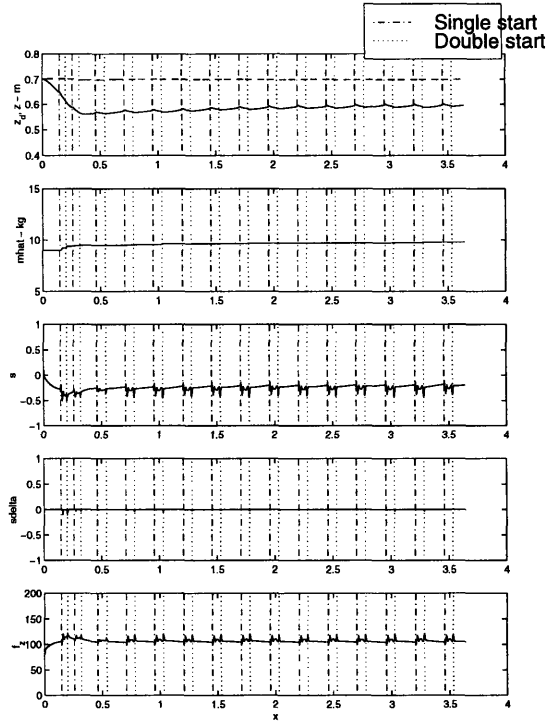


Figure 16. Robust Adaptive Control:  $D = 20$ ,  $\lambda = 2$ ,  $k=50$ ,  $\gamma = 10$ ,  $\hat{m}_o = 9$

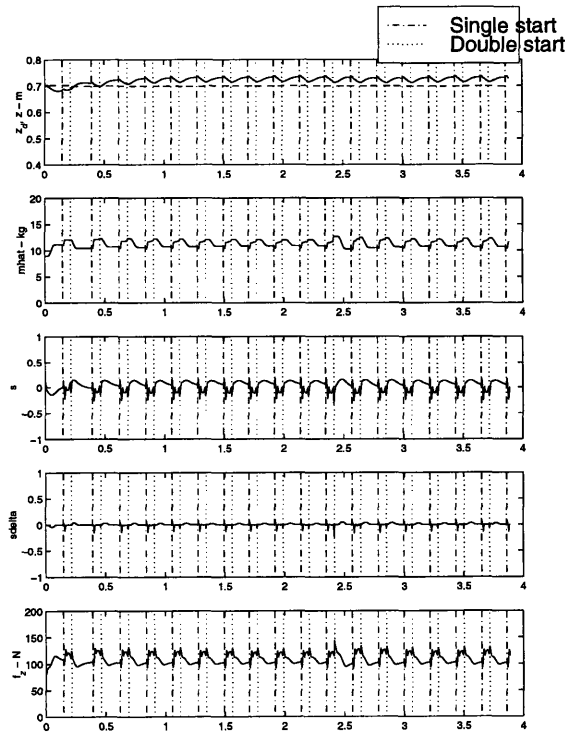


Figure 17. Robust Adaptive Control:  $\gamma = 50$ ,  $\lambda = 2$ ,  $k=50$ ,  $D=5$ ,  $\hat{m}_o = 9$

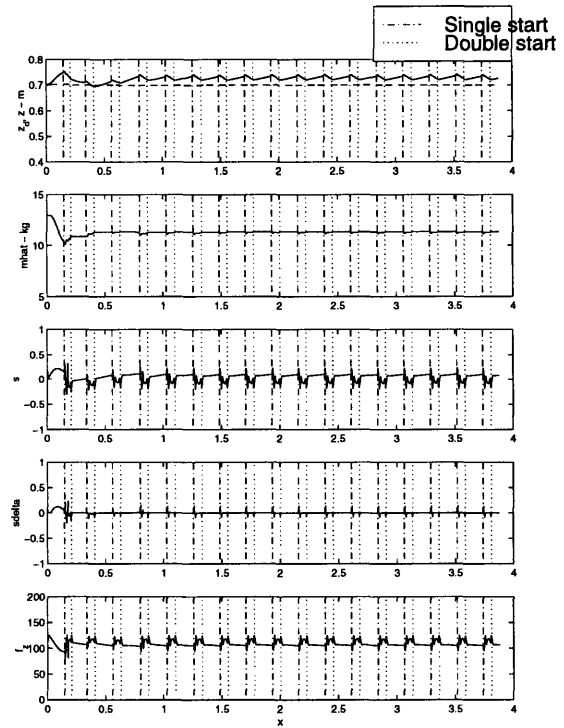


Figure 18. Robust Adaptive Control:  $\hat{m}_o = 13$ ,  $\lambda = 2$ ,  $k=50$ ,  $\gamma = 10$ ,  $D=5$

## 4.5 Discussion

One may ask whether we can simply use PID controller instead of the more complex Robust Adaptive Controller. We would say that a PID controller will probably work fine too. Nonetheless, we think that Robust Adaptive Controller is better because it provides the information of the effective mass. Furthermore, the computation of Robust Adaptive Controller is not very intensive and hence it is worthwhile to implement Robust Adaptive Controller for our purpose. In fact, when the estimation of  $m$  has stopped and all other transient behaviors have settled down, Robust Adaptive Controller behaves like a virtual spring-damper with a constant offset term (Equation (4.14)).

If the legs are heavy, we may split the adaptation parameters into two parts, one for the single support phase and the other for the double support phase because the effective mass for the two phases may deviate substantially from one another.

## 4.6 Conclusion

This chapter has demonstrated successful application of Robust Adaptive Control to biped walking on level ground in the simulation. The effects of the parameters were also studied. It is concluded that Robust Adaptive Controller is applicable for steady biped walking and it enables the biped to adapt to about 18% step change in body mass. The computation requirements for such a controller are very low and do not defeat the original purpose of using the VMC. Thus, Robust Adaptive Controller can be a virtual component candidate for the VMC. Chapter 6 will demonstrate the robustness of this approach by simulating the biped walking over a series of unknown slopes.

# Chapter

## 5 Sloped terrain walking

---

In a totally unstructured environment, the geometry of the terrain is usually very complex. In the study of rough terrain locomotion by a hexapod, [Song and Waldron, 1989] classified the rough terrain into four types of geometric representations: gradient, ditch, vertical step and isolated wall (Figure 19). [Raibert, 1990] said that a terrain can become rough under the following instances: 1) the ground is not level; 2) there is limited traction (slippery); 3) there are areas of poor or nonexistent support (eg., holes).

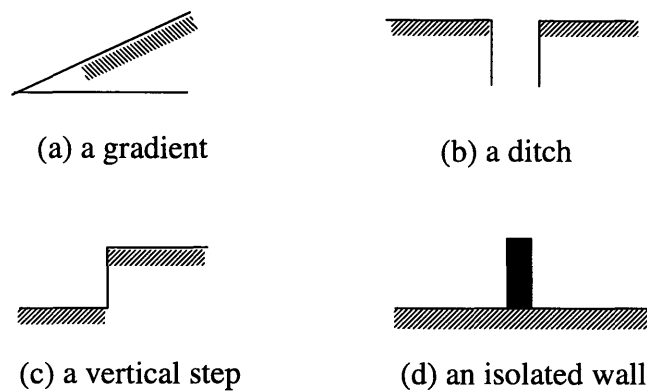


Figure 19. Four typical geometries of terrain: (a) a gradient (b) a ditch (c) a vertical step (d) an isolated wall [Song and Waldron, 1989]

The types of terrain that a biped can overcome depend not only on the relative dimension between the terrain and the biped, but also its mechanism, structure and walking gait. So, when designing a biped, it is very important to take into account the type of terrain it has to overcome. However, this thesis assumes that the biped is already designed and the task is to develop an algorithm for the biped to overcome certain types of rough terrains. This thesis will look only at gradient or sloped terrain. The main objective is to develop a *simple* strategy for sloped terrain walking based on Virtual Model Control (VMC) approach. Based only on geometric considerations, we modified the algorithm for walking on level ground so that the biped can walk on slopes. Last, this thesis also extends the sloped terrain walking strategy to stair climbing. All the simulation results are presented in the next chapter.

## 5.1 Sloped terrain walking using Virtual Model Control

Within a building, be it a commercial, industrial or residential one, the terrain is usually well structured and it can be classified mainly into level ground, slopes and stairs. We will first consider the slopes and extend the application of the VMC to sloped terrain walking. The biped is assumed to be walking on level ground before encountering a slope of unknown transition location and gradient. The biped is just like a blind creature and it should be able to adjust its gait based on its interaction with the slope [Zheng and Shen, 1990].

This thesis assumes that the terrain has no vertical variation along the walking direction and no variation perpendicular to the sagittal plane. The minimum and maximum slope gradients are  $-20^\circ$  and  $+20^\circ$ , respectively. This thesis also assumes that there is no slippage of the feet at all time when they are in contact with the ground.

As mentioned in Chapter 2, the biped in our study has only discrete sensors at the toe and heel to sense the foot's contact with the ground. Together with the joints' position readings, the information provided by these discrete sensors is used to compute the slope gradients at the start of each double support state. The biped will adjust its gait accordingly to continue its stable locomotion on the slope. Since our biped walks dynamically on level ground, we also want it to walk dynamically up or down the slope. The objective is to let the biped adapt to the slope of unknown gradient without complex sensors and algorithm.

When the biped is on a slope and it is in the double support phase, the front and rear supporting legs are resting on different elevations. We call the virtual slope that is formed by joining the ankle of the front and rear legs the *global* slope. The actual slope that each foot is resting on is called the *local* slope. For example, when the back supporting leg is stepping on level ground and the front supporting leg is stepping on an upslope, the local slopes at both legs and the global slope will all have different gradients. In the algorithm, the local and global slope gradients are computed during the double support state.

### 5.1.1 Upslope and downslope walking

This subsection studies the posture of the biped while walking on an upslope and a downslope which have constant gradients. We then decide which parameters or variables should be adjusted so that steady walking can be achieved.

For the biped, the following are some of the possible strategies which can be adopted for slope walking:

1. To adjust the projection of the center of gravity of the biped along the ground. For example, the biped may bend its torso forwards during upslope walking to shift the projection of the center of gravity forwards;
2. To vary the hip height;
3. To change the distance from the front ankle at which the double support phase transits to the single support phase;
4. To vary the horizontal velocity;
5. To vary the step length.

These strategies may be used to improve the walking in one way or another, for example, in terms of stability and energy usage. Some of them may have opposing effects on the slope walking control and this requires optimization methods to obtain an optimal solution. However, we have not yet established a performance index for steady dynamic walking on rough terrain. Therefore we adopt trial-and-error approach to set the parameters for the biped to walk successfully over the sloped terrain. In this preliminary study, since we would like to keep modifications to the level walking algorithm to a minimum, we decide to keep the desired horizontal velocity unchanged and the torso at the same upright posture while the biped walks on the sloped terrain. We also decide to fix the desired step length of the biped along the ground surface regardless of whether it is walking on sloped or level ground. We change only the desired hip height of the biped. We use the *global* slope gradient to modify the desired hip height for walking as described in the next paragraph.

As in the case of level ground walking, the height limit of the biped for upslope is computed based on the desired step length, the distance from the front ankle at which the double support phase transits to the single support phase, and the singularity consideration of the back supporting leg during the double support phase (see Figure 20). Let's denote  $h_{limit}$  to be the hip height limit measured vertically from a global slope. By geometric consideration, the hip height limit  $h_{limit}$  is computed by Equation (5.1).

$$h_{limit} = \sqrt{(l_1 + l_2)^2 - r^2} - r \tan \beta \quad (5.1)$$

where

$$r = s_l \cos \beta + l_t \quad (5.2)$$

Similar to level walking, a factor  $k_{height}$  is multiplied to the height limit  $h_{limit}$  to calculate the desired height of the hip from a global slope. The desired hip height  $z_d$  defined in Section 3.3.3 is then given by Equation (5.3).

$$z_d = k_{height} h_{limit} + x \tan \beta \quad (5.3)$$

where  $x$  is the x-coordinate of the hip with respect to the stance leg's ankle.

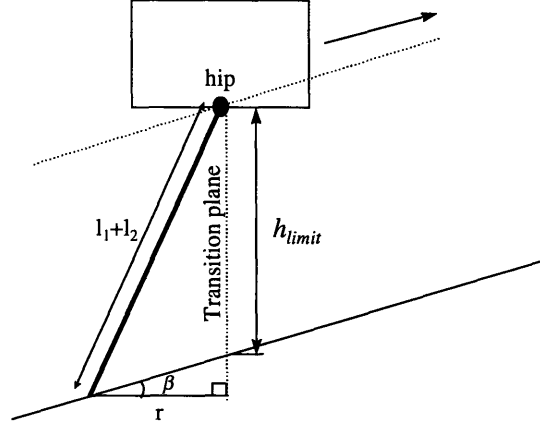


Figure 20. Geometric constraint to calculate  $h_{limit}$ : Level and upslope

For the case of a downslope, both the back supporting leg during the double support phase and the swing leg during the single support phase may reach singular configuration as shown in Figure 21(a) and Figure 21(b), respectively. For the latter case, we assume that the vertical projection of the hip is half way between the front and back supporting legs when the swing leg touches down (see Subsection 3.3.2). Thus, the height limit  $h_{limit}$  is computed as in Equation (5.4).

$$h_{limit} = \sqrt{(l_1 + l_2)^2 - r_1^2} + r_1 \tan \beta \quad (5.4)$$

where

$$r_1 = 0.5s_f \cos \beta \quad (5.5)$$

The minimum of the computed hip height limit  $h_{limit}$  between Equations (5.1) and (5.4) is used to compute the desired hip height  $z_d$  in Equation (5.3) during the downslope walking. These equations can also be used for level walking where  $\beta$  is zero. Note that the foot's dimension is ignored in all computations.



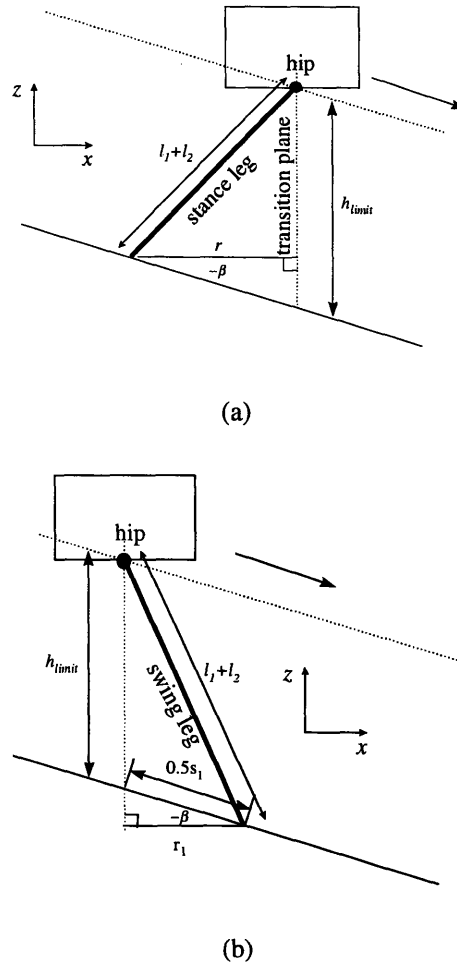


Figure 21. Geometric constraint to calculate  $h_{limit}$  during downslope walking: (a) case 1; (b) case 2

The strategy to control the swing leg control for both the upslope and the downslope walking is the same as that for level ground walking. The step length for the slope walking is measured along the slope and the maximum lift height of the swing leg is measured perpendicular to the slope.

### 5.1.2 Transition cases

This subsection considers transitional walking from level ground to slope and slope to level ground, where the slope can be either ascending or descending. We first discuss the level-to-upslope and downslope-to-level transition.

For level-to-upslope transition, we employ a strategy similar to the one adopted by [Zheng and Shen, 1990]. In their approach, when their biped was walking statically from level ground to an upslope surface, it employed a “compliant” stepping motion when the foot of its swing leg first came into contact

with the sloped surface. The position and orientation of the landing foot were determined by the force information generated by the force sensor underneath the foot at the moment of the contact. The landing foot could then comply with the constraints of the ground. However, the bandwidth of such a strategy is usually small. Thus, it cannot be applied to the dynamic walking of our biped in which large bandwidth control is desirable.

At the moment when the swing foot touches the upslope surface, instead of using the force feedback approach, we set the ankle torque of the swing leg to zero. This allow the swing foot to orient itself and adapt to the slope according to its natural compliance. The whole process is shown in Figure 22. Before the swing foot touches the slope surface, it is swung in the same manner as in level ground walking. When the swing foot toe touches the slope surface (assuming the swing foot's gradient with respect to the level ground is zero initially), the state machine makes a transition from single support to single-to-double transition phase and the ankle torque is set to zero. A sufficiently small angle  $\mu$  between the impact force and the normal of the slope (see Figure 22(a)) will result in an equivalent counter-clockwise moment acting on the foot about the ankle (see Figure 22(b)). The counter-clockwise moment causes the foot to rotate in a counter-clockwise direction until the heel touches down (Figure 22(c)).

This strategy requires the ankle to be as low as possible (preferably below the foot) and  $\mu$  to be small. However, this may not be achievable, for example,  $\mu$  is high if the friction coefficient of the slope surface is high. To enhance the strategy, we add a local PD position control at the ankle to prevent the impact force from turning the foot in a clockwise direction. The swing foot's gradient can also be tilted so that the toe is higher than the ankle.

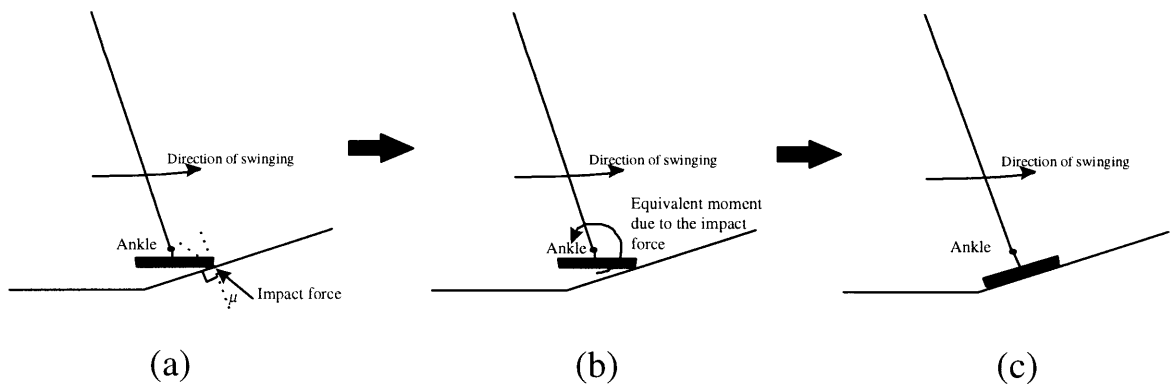


Figure 22. Natural compliance of the swing foot

When both the heel and the toe of the swing foot are on the slope, they trigger the transition from the single-to-double transition phase to the double support phase. The biped then computes the gradient of the *global* slope based on the joints' angles. Note that the global slope gradient is not the same as the real slope gradient since both feet are not on the same slope yet (see Figure 23(a)). The global slope is an imaginary intermediate slope whose gradient is between the level ground gradient (equal to zero) and the actual upslope gradient. However, the biped considers the global slope to be the actual terrain slope during the double support phase. It computes the desired walking height based on the global slope.

When the biped switches to single support phase, it continues to compute the desired walking height based on the global slope. The swing leg trajectory of the single support phase is also planned using the global slope. However, when the biped is at double support phase again, both its legs are on the actual slope and the global slope will have the same gradient as the actual slope (see Figure 23(b)).

Note that during transition walking, the actual step length of the biped may vary significantly from the desired step length. For the level-to-upslope transition, the variation in the step length is due to the premature landing of the swing foot. The biped will reach a steady walking gait as it continues to walk on the same slope. The strategy for the level-to-upslope transition is also applied to the downslope-to-level transition.

In the computation of the desired hip height of the biped, an alternative strategy is to use the local slope gradient instead of the global slope gradient. However, this approach is not good in certain extreme cases. One example is when the biped steps onto a local variation in a terrain (see Figure 24). In this case, if the biped were to use the local slope gradient to compute its desired hip height, the hip would follow trajectory (1) which is steep. That is, the biped may “amplify” the terrain unnecessarily. A drastic action would result even though the actual terrain may not be rough. However, if the intermediate global slope gradient is used, the biped will go along trajectory (2) which is less steep compared to trajectory (1). The usage of the intermediate global slope gradient will allow the biped to have a smoother transition than if it were using the local slope gradient.

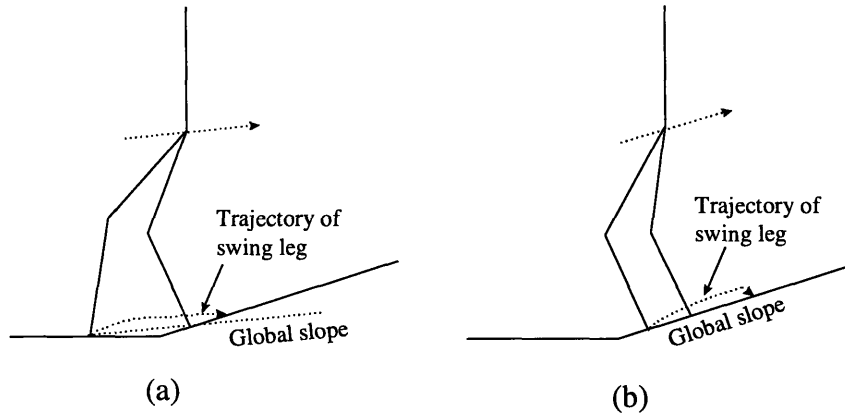


Figure 23. (a) Global slope whose gradient is different from that of the actual slope; and (b) global slope whose gradient is the same as that of the actual slope.

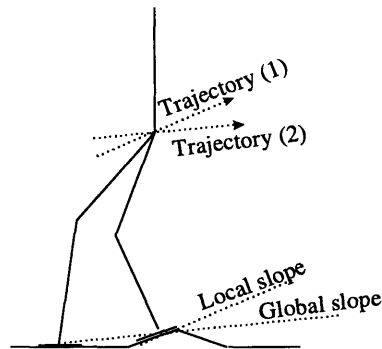


Figure 24. Extreme example to demonstrate a potential problem when the local slope is used to calculate the desired hip height.

This paragraph looks at the level-to-downslope and upslope-to-level transitions. During the level-to-downslope transition, the biped executes the usual walking control for single support phase until the swing time has expired. When the swing time has expired, if the swing foot has not touched down, the biped will exert a preset downwards force exerted at the swing leg's ankle so that the swing foot will continue on its way down. The downwards force will cause the swing leg's ankle to penetrate through a virtual surface (which is the global slope) (see Figure 25(a)). When the virtual surface is penetrated, the biped re-computes the gradient of the *global* slope based on the instantaneous position of the swing leg's ankle (see Figure 25(b)) and adjusts the desired hip height accordingly. This is a continuous process. After the swing leg has touched down<sup>11</sup>, the state machine will switch to the double support state and the biped will compute the intermediate global slope (see Figure 25(c)). In this state, the biped will compute

<sup>11</sup> When both heel and toe's sensors are turned on.

the desired hip height based on the global slope. The swing leg of the next single support state will also follow this global slope. The biped then goes through the whole sequence (Figure 25) again before both feet are on the same slope. The strategy for the level-to-downslope transition can also be applied to the upslope-to-level transition.

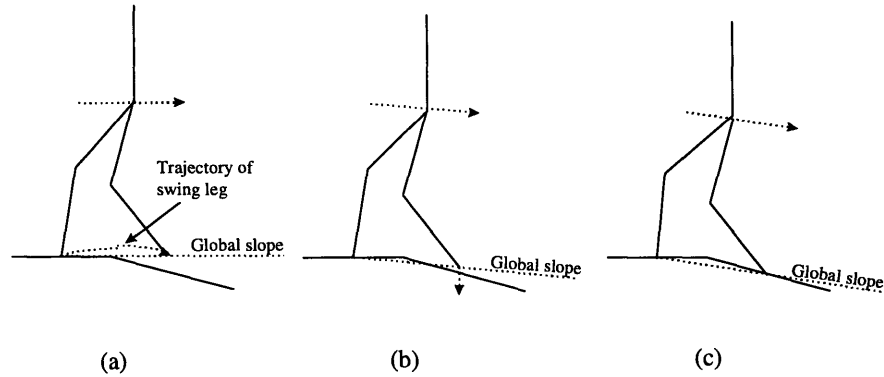


Figure 25. Sequence for level-to-downslope transition

For both the level-to-downslope and upslope-to-level transitions, we have to control the swing leg so that it will not hit the ground prematurely (see swing leg trajectory (1) of Figure 26). To avoid such an event, the desired lift height for the swing leg should be set to a value which will enable it to clear all the edges of the level-to-downslope and upslope-to-level transitions. This is based on the assumption that we know the maximum change in the gradients for each slope transition.

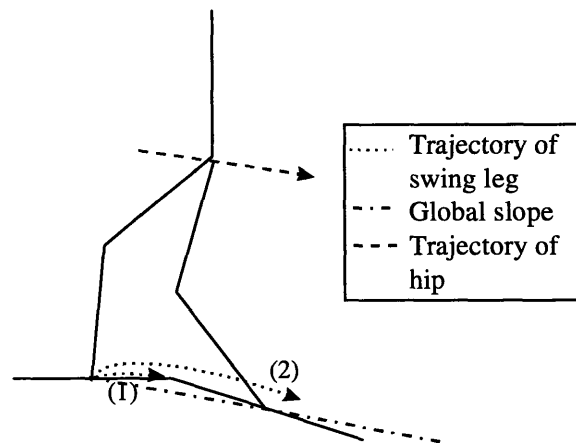


Figure 26. Possible problem with swing leg

For the level-to-downslope and upslope-to-level transitions, the swing leg may land on the edge formed by the intersection of two different slopes. This problem can be solved by several approaches, for

example, by adding more sensors to the feet and adding more event checks in the algorithm; by designing a foot which can accommodate the edge, etc.. This problem will not be studied in this thesis. We assume that all the slope transitions are smooth.

## 5.2 Extension to dynamic stair-walking

The strategies developed for the biped to walk blindly over sloped terrain can be extended to dynamic stair-walking. However, in stair-walking, the biped requires prior knowledge of the stair profile. This is similar to a human who needs to rely on visual capability so that he knows the general location and layout of a flight of stairs before he can walk dynamically on it. The swing leg trajectory needs to be more precise than that for sloped terrain walking since stairs usually have limited foothold area. In our analysis, we assume that the biped can always find a foothold on the stairs.

The concept of global slope is also used in stair-walking (Figure 27). For stair-walking, at the start of the single support phase, the biped will compute a global slope which joins the target ankle position of the swing leg (when the swing foot lands on the desired foothold position) and the stance leg's ankle. This is different from the sloped terrain walking in which the global slope is computed at the beginning of each double support phase.

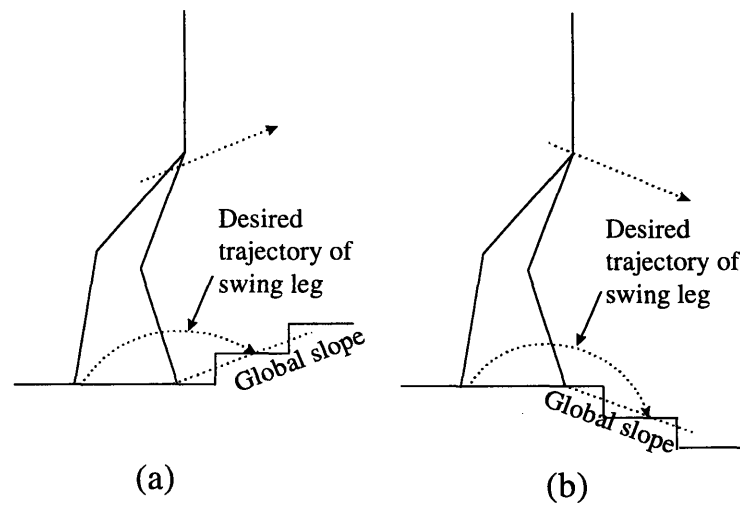


Figure 27. Global slope in stair-walking

# Chapter

## 6 Simulations results

---

This chapter first describes two sloped terrain profiles that were used in the simulation. The simulations' parameters and results of the biped walking on these terrains are also included. The purpose of the simulations was to validate that the strategy developed in the previous chapter could be used to achieve *blind* walking over sloped terrain. The sloped terrain was assumed to have a maximum absolute gradient of  $20^\circ$ .

The robustness of the sloped terrain strategy was also illustrated by simulating the biped walking over a series of random slopes. We had also replaced the vertical virtual component (the one which used a spring-damper) by Robust Adaptive Controller (Chapter 4) and let the biped walk over the same terrain.

In all the simulations, we had assumed no slippage of the biped's feet when they were in contact with the ground and the terrain transition was smooth. We assumed that the feet had shock absorbing material to reduce the effect of impulsive force when it hit the terrain prematurely. We had also assumed perfect actuators at all the joints. Note that the biped did not have any prior information of the terrain's profile. Therefore, it had to *feel* its way through the terrain based on the simple discrete (on/off) sensors at the feet and the joints' position sensors.

### 6.1 Sloped terrain profiles used in the simulations

This section describes two profiles of sloped terrain used in the simulation. In both profiles, we limited the gradient change at terrain transitions to  $20^\circ$ . And we only allow at most one terrain transition per step. The maximum absolute gradient at any point of the terrain was  $20^\circ$ .

We defined sloped terrain *profile one* to be one which consisted of the following sequence of transitions: level-to-upslope, upslope-to-level, level-to-downslope, downslope-to-level, where the upslope and the downslope had gradients of  $20^\circ$  and  $-20^\circ$ , respectively. The profile of this terrain is shown in the top graph of Figure 29. This terrain was used in the simulation so that we could observe and compare the key output variables for the upslope, downslope and transition terrain walking of the biped.

The sloped terrain *profile two* (see the top graph of Figure 31) was rougher than *profile one*. The sloped terrain *profile two* was used to illustrate the robustness of our approach for the biped to walk over a

sloped terrain which consisted of a series of unknown slopes. We had also simulated the biped walking on this sloped terrain profile using Robust Adaptive Controller (Chapter 4).

## 6.2 Walking over the sloped terrain profile one

The purpose of this simulation was to study the walking pattern for upslope, downslope and transitions based on the strategy developed in Chapter 5. The desired values of some of the gaits' variables and the parameters of the virtual components were set as in Table 6. Note that the desired hip height of the biped was computed by the algorithm based on the desired step length and the instantaneous global slope. The initial values of the variables were set to be equal to the desired values in the simulation. Although the desired hip height for level ground walking was computed to be about 0.76m, the initial hip height of the biped was set to 0.68m in the simulation.

Table 6. Desired values of some of the gaits' variables and the parameters of the virtual components set in the simulation

Variable/parameter	Notation	Value
Desired pitch angle of the torso	$\alpha_d$	0 rad
Desired horizontal velocity of the hip	$v_{xd}$	0.4 m/s
Desired step length	$s_l$	0.28 m
Distance from the front ankle at which double support phase transits to single support phase	$l_t$	-0.03m
Desired lift height of swing leg	$h_l$	0.07 m
Parameters of virtual components:		
1. Spring stiffness (in z direction)	$k_z$	1000 N/m
2. Damping coefficient (in z direction)	$b_z$	200 Ns/m
3. Damping coefficient (in x direction)	$b_x$	200 Ns/m
4. Spring stiffness (in $\alpha$ direction)	$k_\alpha$	50 Nm
5. Damping coefficient (in $\alpha$ direction)	$b_\alpha$	20 Nms

Figure 28 shows a stick diagram of the biped walking over the sloped terrain *profile one* from left to right. Figure 29 and Figure 30 show the profiles of the key variables and the joints' torque, respectively. In Figure 29, the vertical "dash-dot" and "dotted" lines represent the start of the single support and the double support phases, respectively. In Figure 30, the vertical "dash-dot", "dotted", "dashed", "continuous" lines represent the start of Right Support, Double Support 2, Left Support and Double Support 1 states, respectively.



The top second graph of Figure 29 shows the discrete changes in the global slope gradient when the biped walked over the terrain. The actual upslope and downslope gradients were  $+0.35$  rad ( $20^\circ$ ) and  $-0.35$  rad, respectively. We could observe that at each of the transition locations (at  $x \approx 0.8, 4.7, 6, 10\text{m}$ ), there was at least one intermediate global slope which had a gradient between the level ground and the actual slope gradient. This helped to provide a “smooth” transition when the biped walked over these transition locations.

The top third graph of Figure 29 shows the actual hip height profile (solid line) of the biped measured from the global slope. This result shows that the biped was able to track the desired hip height (dashed line) within a tolerable range. The ripple found in the actual hip height profile was mainly due to the swing leg dynamics and the variation in the effective mass of the biped as perceived at the hip.

We observe that when the global slope gradient was negative, the desired hip height<sup>12</sup> (dashed line in the top third graph of Figure 29) of the biped was higher than when the global slope gradient was positive. This was the result of the geometric considerations (subsection 5.1.1) when we computed the desired hip height of the biped.

For the level-to-upslope transition, a substantial lowering of the desired hip height (from  $0.76$  m to  $0.68\text{m}$ , see Figure 29) helped in the transition because the dynamic tendency of the biped at the moment before its swing foot hit the upslope was to travel horizontally. This lowering of the desired hip height helped to prevent drastic changes in the vertical virtual force  $F_z$  required to divert the biped to walking along the upslope. We can observe in the same graph that the transitional variation in the actual hip height (between  $x = 0.5$  m and  $1.5$  m) during this transition was quite smooth.

For the upslope-to-level transition, the change from low to high (from  $0.68$  m to  $0.76$  m) in the desired hip height of the biped relative to the global slope also helped to smooth the transition. This could be explained by the same dynamic behavior as in the previous paragraph. The transitional variation in the actual hip height of the biped (between  $x = 4.5$  m and  $5.5$  m) was also observed to be smooth.

For level-to-downslope transition, we observed that the variation in the desired hip height (around  $x = 6.2$  m) was not very large. However, the variation in the vertical virtual force  $F_z$  was very large. This might have been due to the discontinuous change in the desired hip’s trajectory.

For downslope-to-level transition, the variation in the vertical virtual force  $F_z$  was not so large. The impact of the swing leg when it hit the level ground could have provided an impulse which happened to assist in the discontinuous change of the desired hip’s trajectory.

---

<sup>12</sup> Relative to the global slope.

From the horizontal velocity profile of the hip ( $\dot{x}$  vs  $x$ ) in Figure 29, we observed that the velocity fluctuation was higher for the upslope walking than for the downslope walking. This was mainly due to two causes. First, the dynamic frequency of the biped during the single support phase<sup>13</sup> was higher for the upslope walking than for the downslope walking. This is because the hip height of the biped (measured from the slope) was lower in the former. Thus, for the upslope walking, the horizontal velocity of the hip increases at a rate relatively faster after the vertical projection of the biped's center of gravity crossed over its stance ankle during the single support phase.

The swing leg trajectory was the second cause for the difference in the velocity profile. We observed from the stick diagram that the swing leg had different trajectories for the upslope, downslope and level walking. Hence, the dynamic disturbance of the swing leg for each of the cases were also different. This resulted in different velocity profiles for the three cases. For example, in the upslope walking, the swing leg started from a configuration which was closer to the singular configuration (ie., fully straightened), thus causing higher disturbance to the horizontal velocity.

The horizontal velocity also deviated significantly from the desired value at the upslope-to-level transition and the level-to-downslope transition. This was mainly due to the fact that the biped took additional time to *feel* the ground at these locations during the single support phase. This delay in step time resulted in slightly higher horizontal velocity when the biped reached the next double support phase. We also observed the horizontal hip velocity, just after the touch down of the swing leg, was a fraction of the velocity just before the touch down. This was due to the impact effect of the swing leg when it touched down [Kajita and Tani, 1991].

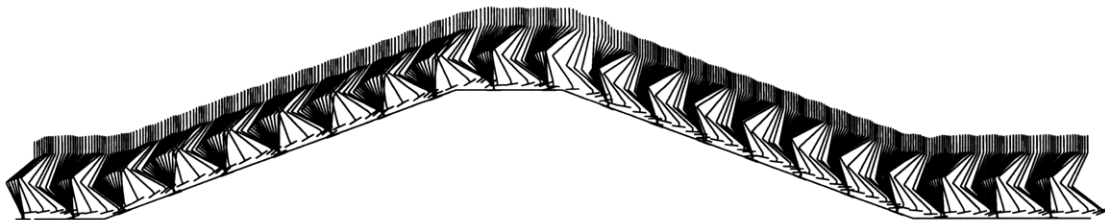


Figure 28. Stick diagram of the biped walking over the sloped terrain *profile one* from left to right (spaced approximately 0.08 s apart and showing only the left leg)

---

<sup>13</sup> Similar to an inverted pendulum.

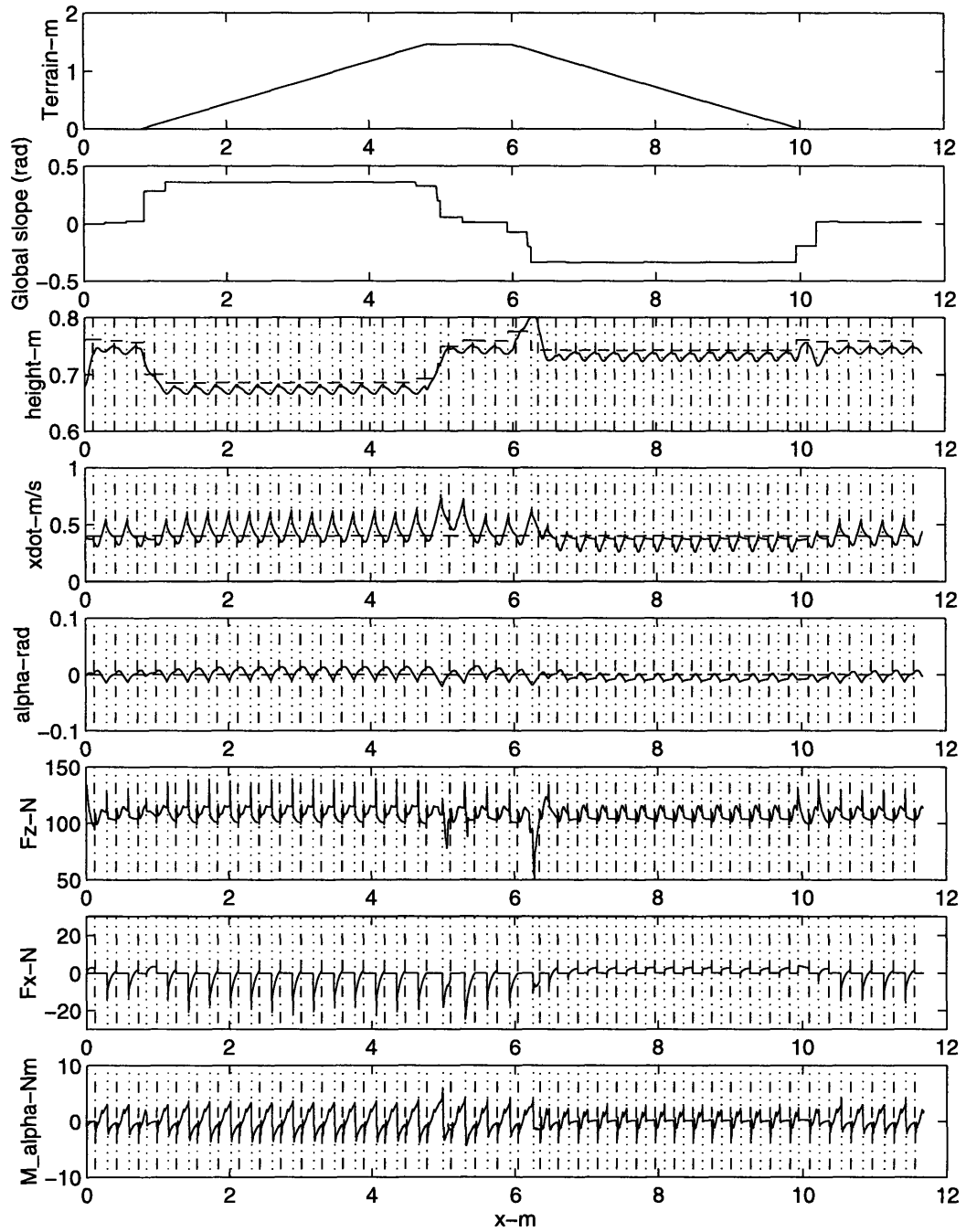


Figure 29. Profiles of the key variables when the biped walked over the sloped terrain *profile one*

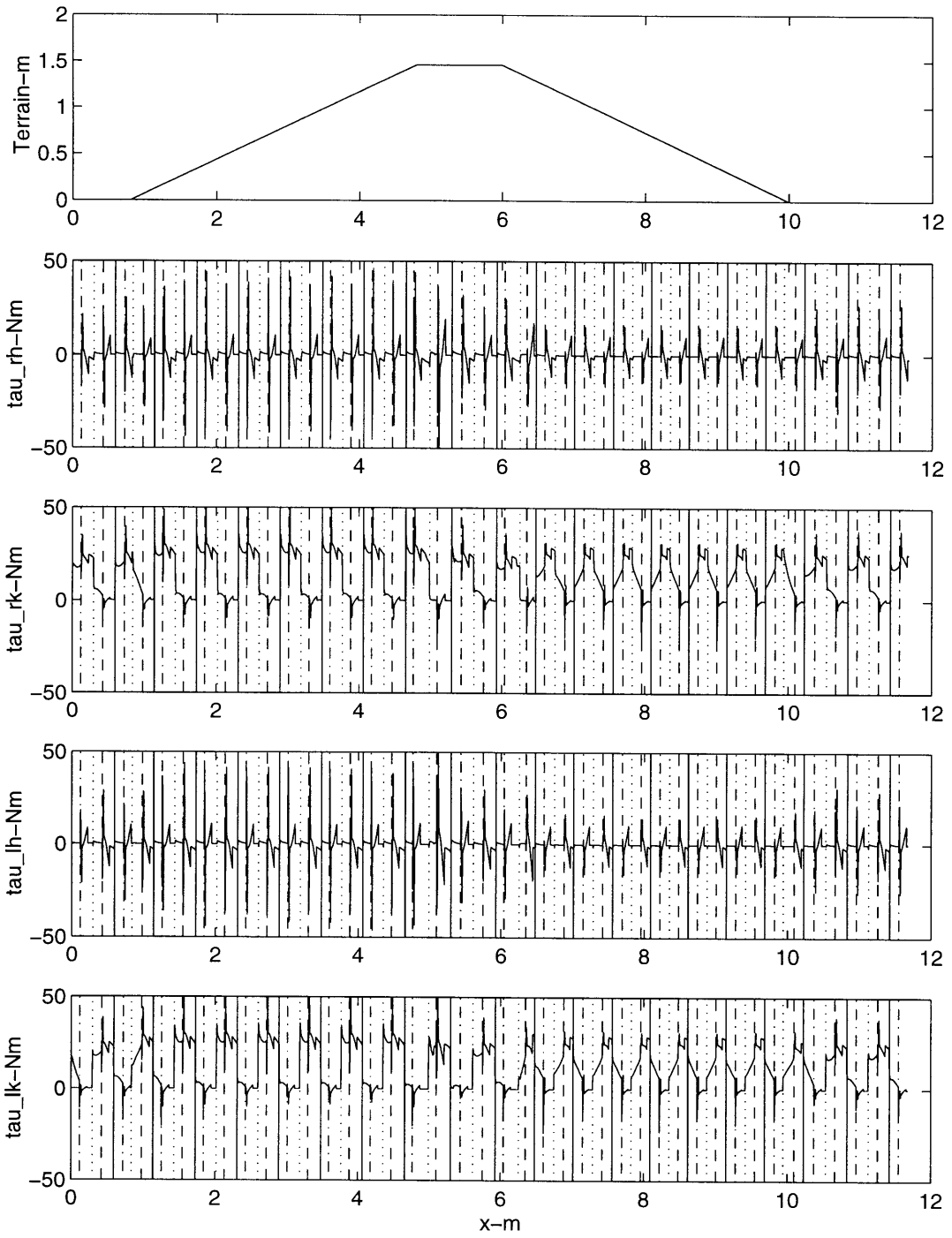


Figure 30. Torque profiles of the hip and the knee joints when the biped walked over the sloped terrain *profile one*

### 6.3 Walking over the sloped terrain profile two

The purpose of this terrain profile was to demonstrate the robustness of the strategy developed for sloped terrain walking. The desired values of some of the gait variables and the parameters of the virtual components were set as in shown Table 6. The initial values of the variables were set to be equal to the desired values in the simulation. The initial hip height was set to 0.64m and this is the same as the desired hip height for walking on level ground. Figure 31 shows the profiles of the key variables. The vertical “dash-dot” and “dotted” lines represent the start of the single support and double support phases, respectively.

Note that the profile of the terrain was not known to the biped in advance. The biped was required to *feel* its way through the terrain. From Figure 31, we observed that the biped could cope with this rougher terrain without much difficulty. The actual hip height, hip horizontal velocity and pitch angle of the torso were well-behaved in the simulation.

Based on the analysis in Chapter 4, we replaced the vertical virtual spring-damper with Robust Adaptive Controller. The following parameters:  $\lambda = 2$ ,  $k=100$ ,  $\gamma =10$ ,  $D=5$ ,  $\hat{m}_o =9$ , were used for Robust Adaptive Controller; the other parameters and the desired values of the gaits' variables were the same as those listed in Table 6 except for  $l_r$  (the distance from the front ankle at which the double support phase transits to the single support phase) which was set to 0.03m. The initial values of the pitch angle of the torso and the horizontal hip velocity were set to be equal to the desired values in the simulation. The hip height was set to 0.7m initially. The biped was assumed to start from Double Support 1 state.

The simulation result of the biped walking on sloped terrain *profile two* is shown in Figure 32. It showed that the biped walking using Robust Adaptive Controller was comparable with the previous implementation which used only springs and dampers. However, compared to the previous implementation where the average horizontal velocity of the hip was generally lower than the desired value, this implementation had higher velocity than the desired value. This was mainly due to the fact that we had set  $l_r$  (the distance from the front ankle at which double support phase transits to single support phase) to a new value (0.03m) in this implementation instead of previous value (-0.03m).

We observed that the estimated mass  $\hat{m}$  did not converge to a constant value. It was because at the beginning of most of the double support phases, the actual hip heights of the biped deviated slightly and randomly from the desired hip heights. The randomness of the deviations was due to the randomness of the terrain. Robust Adaptive Controller was not configured to identify or ignore such error signals. Hence it tried to adapt to them. As long as the parameters of Robust Adaptive Controller were properly

selected, for example, choosing a high value for the bound  $\phi$ , the overall performance of such implementation should still be robust.

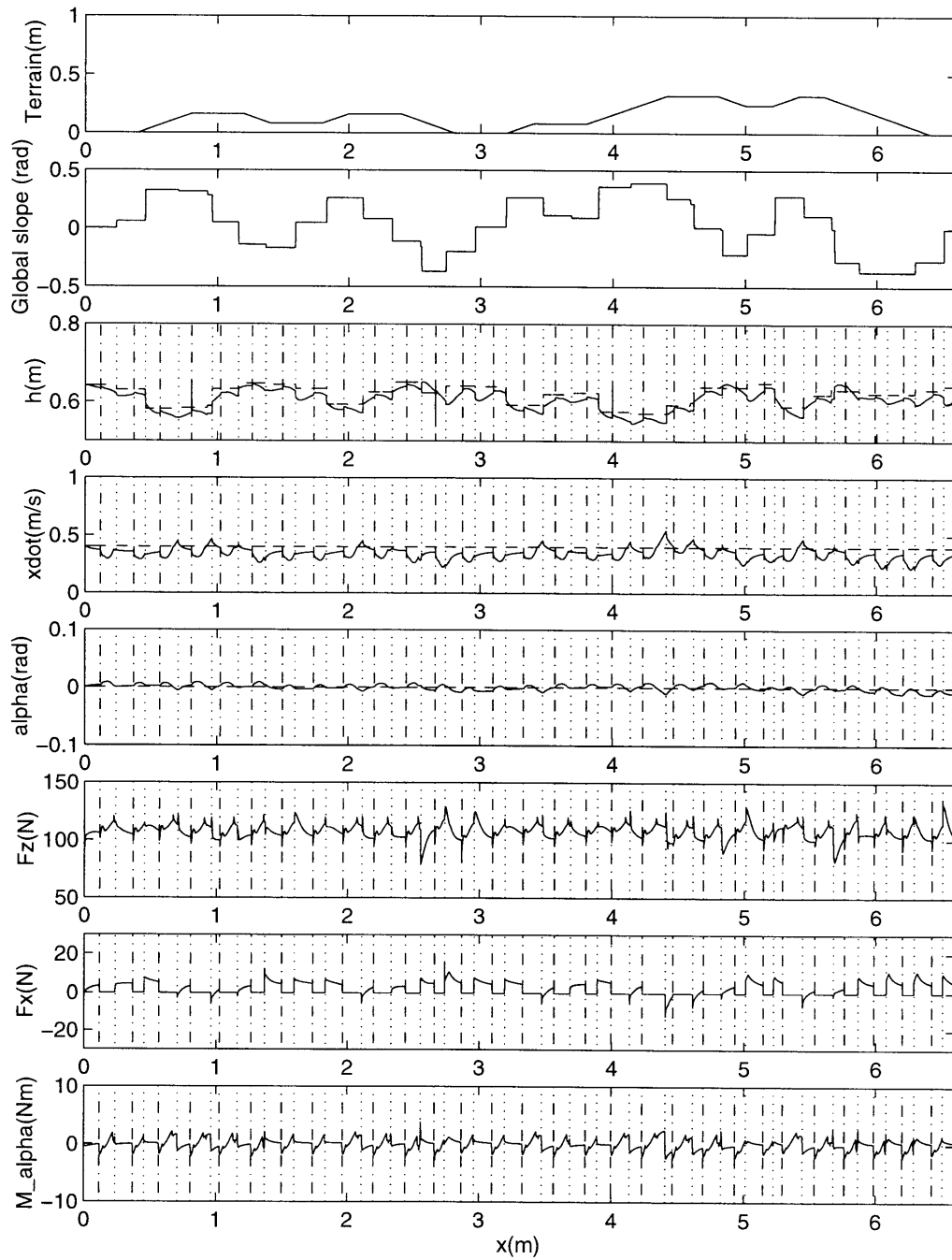


Figure 31. Profiles of the key variables when the biped walked over sloped terrain *profile two*

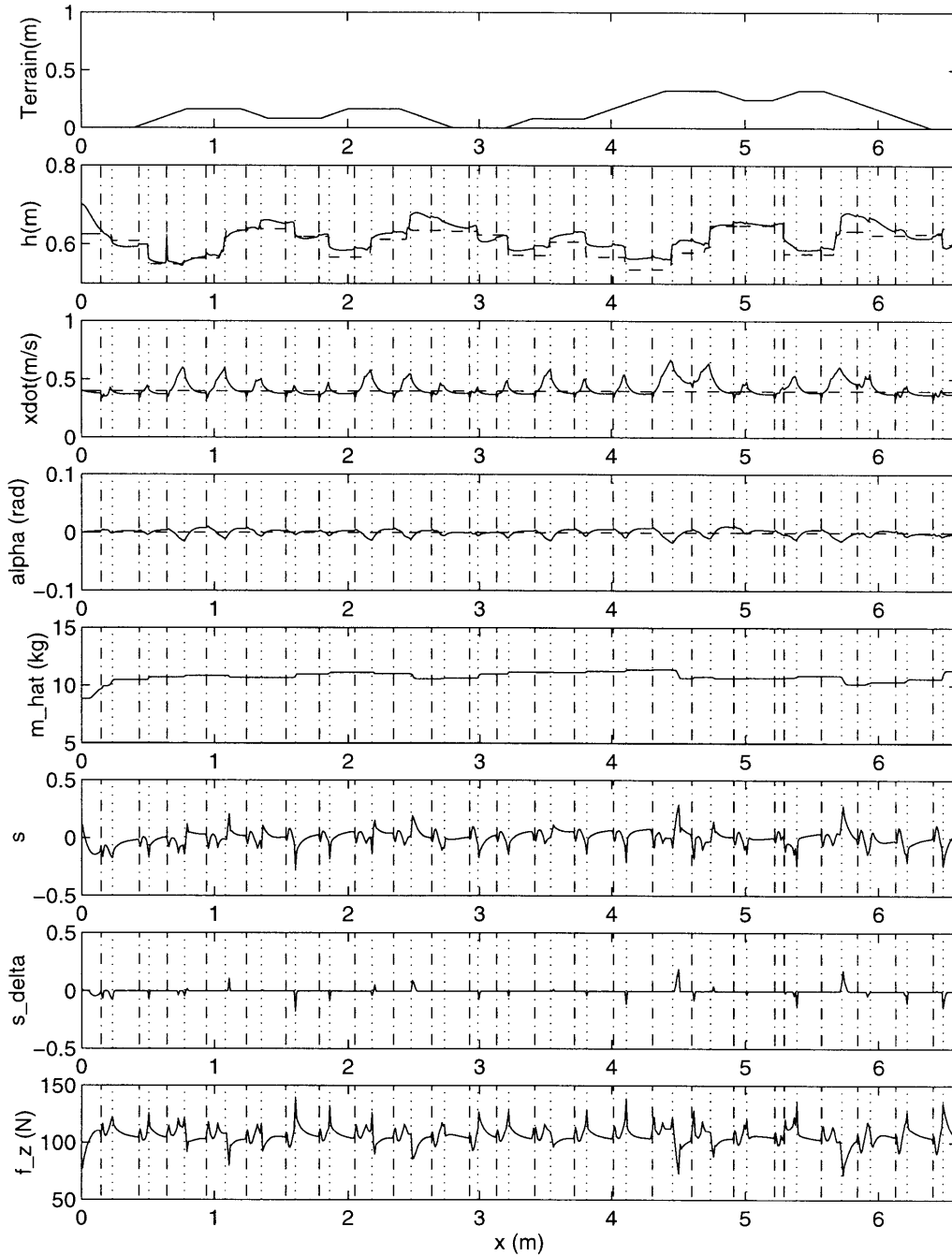


Figure 32. Variables' profiles of the biped walking over the sloped terrain *profile two* using Robust Adaptive Controller as the vertical virtual component ( $\lambda = 2, k=100, \gamma =10, D=5, \hat{m}_o=9$ )

## 6.4 Walking on stairs

In this section, the simulation results of a stair-walking are included. The selected stair profile is shown in the first graph of Figure 34. Each step of the stairs was 0.1m in vertical variation and 0.25m in horizontal width. The biped was assumed to know the profile of the stairs in advance. The desired variables and the parameters were set as shown in Table 6 except for the desired horizontal velocity of the hip and the lift height. The desired horizontal velocity of the hip was reduced to 0.2m/s since the slope of the stairs was quite steep. The lift height  $h_l$  was set to 0.1m for level ground walking and 0.2m for stair-walking. In the simulation, the initial value of the pitch angle of the torso and the horizontal velocity of the hip were set to the desired values. The initial hip height was set to 0.74m. The biped was assumed to start from Double Support 1 state.

Figure 33 shows the stick diagram (only the left leg is shown) of the biped walking over the stairs from left to right. Figure 34 shows the profiles of the key variables. The vertical “dash-dot” and “dotted” lines in Figure 34 represent the start of single and double support phases, respectively. The key output variables were well-behaved and thus validated the applicability of the *global slope* concept to stair-walking. Note that there was no intermediate global slope which existed in sloped terrain walking. We could have also incorporated in stair-walking some intermediate global slopes at the transition locations to smoothen the transitions.

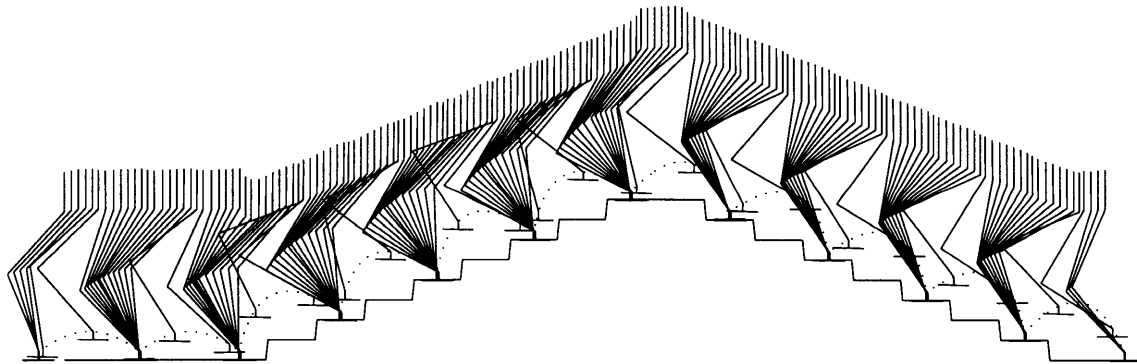


Figure 33. Stick diagram of the biped walking on the stairs (spaced approximately 0.2 s apart and showing only the left leg)



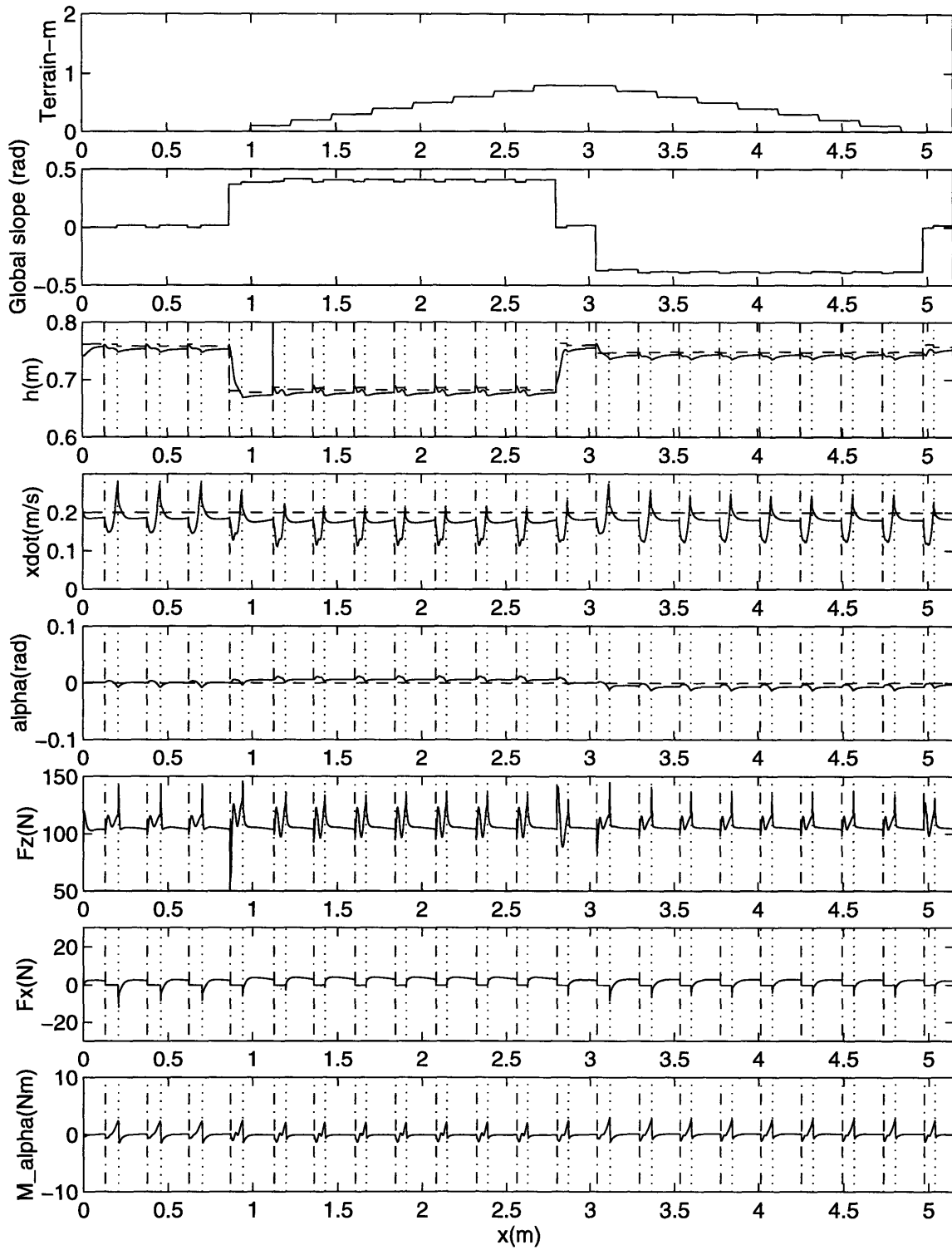


Figure 34. Output variables profiles of the biped walking over the stairs

## 6.5 Discussion

This chapter has demonstrated by simulation that a planar biped is capable of walking blindly over a two-dimensional random sloped terrain using virtual spring and damper components. The notion of *global slope* was used to plan the desired trajectory of the biped's hip. The natural compliance of the swing foot was also used for the swing foot to orientate itself along the *local slope* during touch down. As long as the maximum absolute gradient of the sloped terrain and the maximum transitional change in the gradient are below certain limits, the strategy developed for the sloped terrain walking can result in stable walking.

To apply the level walking algorithm for sloped terrain walking, we modified the algorithm based on the geometry. Given a desired step length, we let the biped walk with the body as high as possible without causing the legs to reach singular configurations. This resulted in a desired body height which varied with the slope gradient. This is different from [Kajita and Tani, 1991] approach in which the body height of the biped was fixed regardless of the slope gradient.

Virtual Model Control (VMC) approach results in a motion similar to the *Linear Inverted Pendulum* mode described in [Kajita and Tani, 1995]. In the latter, a linear trajectory (or constraint line) was formed based on the projected foothold position of the swing leg. A simple dynamic equation based on a massless leg model of the biped was used to obtain the dynamics of the biped travelling along the constraint line. However, to realise the constraint control, Kajita and Tani used inverse kinematics and applied local position feedback at the joints. In the VMC, we do not need to solve any inverse kinematics and inverse dynamics of the biped [Pratt, 1995]. We simply let the virtual components generate the required cartesian forces. These forces are then transformed by a matrix to the joints' torque. If the biped had massless legs, the VMC using the virtual components described in Section 3.3 would also generate a linear trajectory in cartesian space. In the VMC, the resulting equations for controlling the biped are even simpler than those used in [Kajita and Tani, 1995] but we need to use some intuition in the former case. Nonetheless, both approaches have shown that we do not need to have a complex control algorithm in order to control a biped to walk dynamically on level or sloped ground.

In the VMC, the biped behaves as if there is a passive suspension between the ground and the biped's body. For sloped terrain which we assume to have no vertical step variation along its path, it is not required to have *active suspension*<sup>14</sup> described by [Raibert, 1986a]. The biped simply tries to swing the leg to achieve a desired step length, but if the swing leg prematurely hits a slope surface, the actual step

---

<sup>14</sup> [Raibert, 1986a] used this term to explain the advantage of a legged machine that it could choose a foothold location so that the body would be decoupled from the unevenness of the terrain.

length will be shorter than the desired value. When this happens, the biped will go to the next single support phase earlier. This is just how a human will react when he walks up a ramp from a level surface blind-folded. Hence, for the sloped terrain, we do not need to know the terrain profile in advance. However, for stair-walking, the active suspension approach is required since the biped cannot place its swing foot arbitrarily on the terrain. This is the same for humans. We will not be able to walk dynamically on stairs without knowing their general location, layout, and approximate size. However, humans are much more advanced in that we do not need to know the *exact* dimensions of the stairs to walk steadily over them.

There are still a number of future areas to be addressed. One of which is the effect of the swing leg dynamics and its disturbance on the body during the single support phase. It will also be interesting to compare various walking postures and their effects. For example, we might want to change the bending direction of the legs and study its effect on sloped terrain walking.

We are also looking at the usage of the ankle torque to assist the walking. For example, it can be used to control the horizontal velocity to a limited extent [Kajita and Tani, 1995]. Besides using the ankle, there are also a few other means of controlling the horizontal velocity. We should try to find out which of them are effective and under which conditions they are effective.

We need to study the effect of changing other gait parameters like the torso pitch, desired horizontal velocity, double to single support transition distance, step length, etc., on the stability of slope walking. However, we will first need to define a performance index for rough terrain walking.

We had assumed in the simulations that there was no slippage problem. In real application, we foresee a good foot design and a good swing leg control will be necessary so that slippage will not occur in the real implementation.

Although the study was limited to a planar biped, the information obtained would still be useful for 3-D walking since the dominant walking dynamics of a biped happens in the sagittal plane [Raibert, 1986a]. If we can decouple partially or completely the frontal plane motion from the sagittal plane motion, we should be able to use the algorithm developed in this thesis for 3-D walking bipeds.

The VMC approach may not be the best and definitely not the only approach, but it is very simple to implement. Most importantly, most of the parameters and variables of the VMC approach possess some intuitive sense. This has compensated for the weakness of the VMC that it does not utilise the dynamic equations of the system for control. However, its present approach (using spring-damper as the virtual components) may not be applicable to transient motion control which generally requires either dynamic or energy information of the system.

# Chapter

## 7 Conclusions and Further Work

---

### 7.1 Conclusions

This thesis has demonstrated the successful simulation of the application of Virtual Model Control (VMC) to a seven-link planar biped for it to walk *dynamically* and *steadily* over sloped terrain with unknown slope gradients and transition locations. It assumed that the slope gradients were between  $-20^\circ$  and  $+20^\circ$ ; and the sloped terrain had maximum transitional gradient change of less than  $20^\circ$ . The developed algorithm for sloped terrain walking was based on the level ground implementation and only minor changes were needed. In the implementation, a *virtual surface* was defined using a *global slope* computed at the beginning of each double support phase. The algorithm then computed the desired hip height based on the global slope and resulted in a straight line trajectory parallel to the virtual surface. It was very simple to implement and did not require an extensive sensory system to achieve blind walking. The main knowledge required for the implementation was intuition and geometric considerations. The plausibility of the VMC approach to control the biped to walk steadily and dynamically over unknown sloped terrain without any dynamics computation may seem too good to be true. This coincides with a statement made by M. Raibert [Raibert, 1990]: “A *legged system can exhibit complicated dynamic behavior without requiring a very complicated control system.*”

We have also replaced the vertical virtual spring-damper with Robust Adaptive Controller which was successfully implemented for the biped to walk over random sloped terrain. This thesis has also shown how the algorithm for sloped terrain walking can be modified so that it can be used for the stair climbing task.

### 7.2 Further Work

To refine the algorithm further, we will formulate a performance index for sloped terrain walking. Based on such an index, we can then implement some optimization or learning control techniques for the biped to select a good set of variables for robust sloped terrain walking.

We will also apply the algorithm developed in this thesis to 3-D walking. To achieve this, we will need to design a 3-D biped whose frontal plane motion control can be decoupled partially or completely from the sagittal plane motion.

# Appendix A:

## Equations to convert virtual forces to joints' torque

---

### A.1 Double Support Phase

The equations to convert virtual forces to joints' torque during the double support phase was derived in [Pratt, 1995] as shown in Equation A.1. Note that the subscript  $l$  denotes the left leg and  $r$  denotes the right leg and the sign convention is shown in Figure A.1:

$$\begin{bmatrix} \tau_{lk} \\ \tau_{lh} \\ \tau_{rk} \\ \tau_{rh} \end{bmatrix} = \begin{bmatrix} \frac{CV}{E} & \frac{DV}{E} & \frac{V+QD-RC}{2E} + \frac{1}{2} \\ 0 & 0 & +\frac{1}{2} \\ -\frac{AW}{E} & -\frac{BW}{E} & \frac{-W-SB+TA}{2E} + \frac{1}{2} \\ 0 & 0 & \frac{1}{2} \end{bmatrix} \begin{bmatrix} F_x \\ F_z \\ M_\alpha \end{bmatrix} \quad (\text{A.1})$$

where

$$\begin{aligned} A &= -L_1 \cos \theta_{la} - L_2 \cos(\theta_{la} + \theta_{lk}) \\ B &= -L_1 \sin \theta_{la} - L_2 \sin(\theta_{la} + \theta_{lk}) \\ C &= -L_1 \cos \theta_{ra} - L_2 \cos(\theta_{ra} + \theta_{rk}) \\ D &= -L_1 \sin \theta_{ra} - L_2 \sin(\theta_{ra} + \theta_{rk}) \\ E &= CB - AD \\ Q &= -L_2 \cos(\theta_{la} + \theta_{lk}) \\ R &= -L_2 \sin(\theta_{la} + \theta_{lk}) \\ S &= -L_2 \cos(\theta_{ra} + \theta_{rk}) \\ T &= -L_2 \sin(\theta_{ra} + \theta_{rk}) \\ V &= QB - RA \\ W &= SD - TC \end{aligned}$$

### A.2 Single support phase

In the single support phase, due to the limp joint at the ankle, one of the virtual forces due to the virtual components cannot be implemented. In the actual implementation, we only adopt the vertical and torsional motion control. The relation between the virtual force vector and the torque vector is shown by Equation (A.2) [Pratt, 1995]:

$$\begin{bmatrix} 0 \\ \tau_k \\ \tau_h \end{bmatrix} = \begin{bmatrix} -L_1 \cos \theta_a - L_2 \cos(\theta_a + \theta_k) & -L_1 \sin \theta_a - L_2 \sin(\theta_a + \theta_k) & 1 \\ -L_2 \cos(\theta_a + \theta_k) & -L_2 \sin(\theta_a + \theta_k) & 1 \\ 0 & 0 & 1 \end{bmatrix} \begin{bmatrix} F_x \\ F_z \\ M_\alpha \end{bmatrix} \quad (\text{A.2})$$

We simply allow the vertical virtual force  $F_z$  and the rotational virtual force  $M_\alpha$  to influence the horizontal motion. The first row of Equation (A.2) generates Equation (A.3) which shows the equivalent

horizontal virtual force on the biped's hip if the vertical virtual force  $F_z$  and the rotational virtual force  $M_\alpha$  were to be implemented in the single support phase.

$$F_x = -\frac{1}{L_1 \cos \theta_a + L_2 \cos(\theta_a + \theta_k)} \begin{bmatrix} L_1 \sin \theta_a + L_2 \sin(\theta_a + \theta_k) & -1 \end{bmatrix} \begin{bmatrix} F_z \\ M_\alpha \end{bmatrix} \quad (\text{A.3})$$

The Equation (A.4) [Pratt, 1995] was used to compute the hip and knee joints' torque in the single support phase.

$$\begin{bmatrix} \tau_k \\ \tau_h \end{bmatrix} = \begin{bmatrix} \frac{-L_1 L_2 \sin \theta_k}{L_1 \cos \theta_a + L_2 \cos(\theta_a + \theta_k)} & \frac{L_1 \cos(\theta_a)}{L_1 \cos \theta_a + L_2 \cos(\theta_a + \theta_k)} \\ 0 & 1 \end{bmatrix} \begin{bmatrix} F_z \\ M_\alpha \end{bmatrix} \quad (\text{A.4})$$

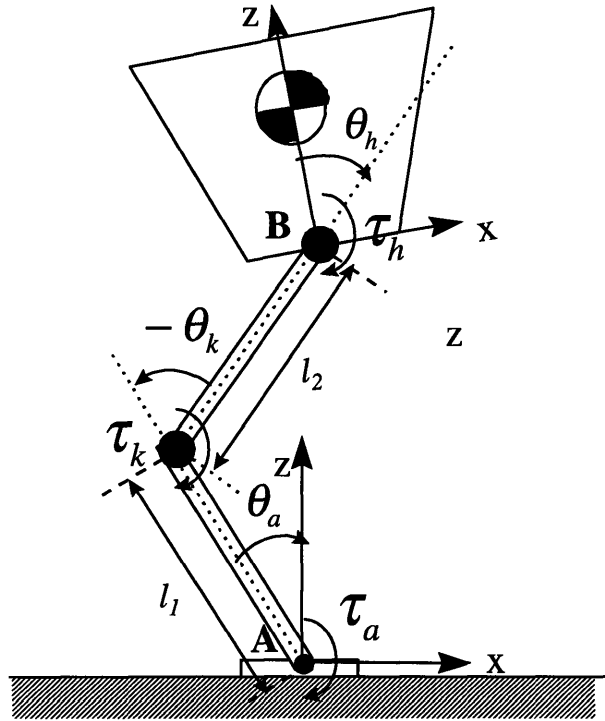


Figure A.1. The notations and sign convention

## Appendix B: Stability analysis based on “massless legs” model

---

This appendix analyzes the stability of Virtual Model Control (VMC) application (as described in Section 3.3) to steady dynamic walking of the biped. Since the masses of the biped’s legs are small compared to the body mass, we reduce the model to one which has massless legs as shown in Figure B.1. We have also ignored the transition phases because they are very similar to the single support phases. Let  $[x, z, \alpha]^T$  be the generalized coordinates which locate the cartesian frame  $ox_bz_b$  attached to the body with respect to the inertia cartesian frame  $OXZ$ ,  $[F_x, F_z, M_\alpha]^T$  be the generalized forces and  $[d_x, d_z, d_\alpha]^T$  be the disturbances (e.g. due to the impact during the touch down of the swing leg) along each of the generalized coordinates. Also, let the body mass and moment of inertia (about the center of mass) be  $m$  and  $I$ , respectively. The center of mass of the body is at distance  $l$  from the hip. The resultant dynamic equations of motion are simply

$$m\ddot{x} = F_x + d_x \quad (\text{B.1})$$

$$m\ddot{z} = F_z - mg + d_z \quad (\text{B.2})$$

$$\begin{aligned} I\ddot{\alpha} &= M_\alpha + F_x l \cos \alpha + F_z l \sin \alpha + d_\alpha \\ &= M_\alpha + ml \cos \alpha \ddot{x} + (m\ddot{z} + mg)l \sin \alpha + d_\alpha \end{aligned} \quad (\text{B.3})$$

In matrix form, they can be represented as follows

$$\begin{bmatrix} F_x \\ F_z \\ M_\alpha \end{bmatrix} = \begin{bmatrix} m & 0 & 0 \\ 0 & m & 0 \\ -ml \cos \alpha & -ml \sin \alpha & I \end{bmatrix} \begin{bmatrix} \ddot{x} \\ \ddot{z} \\ \ddot{\alpha} \end{bmatrix} + \begin{bmatrix} 0 \\ mg \\ -mgl \sin \alpha \end{bmatrix} + \begin{bmatrix} d_x \\ d_z \\ d_\alpha \end{bmatrix} \quad (\text{B.4})$$

The control laws based on the virtual components described in Section 3.3 are listed as follows

$$F_x := b(\dot{x}_d - \dot{x}) \quad (\text{B.5})$$

$$F_z := k_z(z_d - z) + b_z(\dot{z}_d - \dot{z}) \quad (\text{B.6})$$

$$M_\alpha := k_\alpha(\alpha_d - \alpha) + b_\alpha(\dot{\alpha}_d - \dot{\alpha}) \quad (\text{B.7})$$

where  $\dot{x}_d$ ,  $z_d$  and  $\alpha_d$  are the desired horizontal velocity of the hip, the desired hip height and the desired body pitch angle, respectively.

We can apply Modern Control theory to analyze the stability of such a system. However, it is less complex if we analyze the stability in each coordinate separately, especially for  $x$  and  $z$ , where the resulting closed loop equations are decoupled from other coordinates.

For the vertical height control, we substitute Equation (B.6) into (B.5) and this gives

$$m\ddot{z} = k_z(z_d - z) + b_z(\dot{z}_d - \dot{z}) - mg + d_z \quad (\text{B.8})$$

Without loss of generality, let's neglect  $mg$ . Rewriting Equation (B.8) in Laplace transformed form, assuming zero initial conditions, we obtain

$$Z(s) = \frac{k_z + b_z s}{ms^2 + b_z s + k_z} Z_d(s) + \frac{1}{ms^2 + b_z s + k_z} D_z(s) \quad (\text{B.9})$$

Since  $m$ ,  $b_z$  and  $k_z$  are strictly positive, this coordinate is stable (with closed loop poles lying in the left half of the  $s$ -plane). Also, the disturbance due to impact will be attenuated if its frequency is higher than the bandwidth of the closed loop system along the  $z$  direction.

For the horizontal velocity control, considering for the double support phase that the horizontal virtual damper can be applied, we obtain the following equation by substituting Equation (B.5) into Equation (B.1)

$$m\ddot{x} = b_x(\dot{x}_d - \dot{x}) + d_x \quad (\text{B.10})$$

Since the input is velocity, we take the Laplace transform of Equation (B.10) (assuming zero initial conditions) with respect to velocity  $v_x$  and obtain the following

$$V_x(s) = \frac{b_x}{ms + b_x} V_{xd}(s) + \frac{1}{ms + b_x} D_x(s) \quad (\text{B.11})$$

Equation (B.11) shows that the horizontal velocity is stable and it converges to the desired velocity. However, during the single support phase, we are not able to control this parameter. Therefore, we can only say that this parameter will not diverge if the double support phase is sufficiently long to correct the error in velocity resulting from the single support phase. We may also use other horizontal velocity control methods, for example, by varying the foot placement of the swing leg.

For the pitch angle control, we use the third dynamic equation (Equation (B.3)). Note that the third dynamic equation is nonlinear and there is coupling among the generalized coordinates:  $x$ ,  $z$  and  $\alpha$ . However, since we are keeping the body upright throughout the walking cycle, we can linearize the



equation about  $\alpha = 0$ . After substituting the control law (Equation (B.7)) into Equation (B.3) and linearizing the resulting equation about  $\alpha = 0$ , the following equation is obtained

$$I\ddot{\alpha} = k_{\alpha}(\alpha_d - \alpha) + b_{\alpha}(\dot{\alpha}_d - \dot{\alpha}) + F_x l + d_{\alpha} \quad (\text{B.12})$$

By taking the Laplace transform of Equation (B.12) (assuming zero initial conditions), we have

$$A(s) = \frac{k_{\alpha} + b_{\alpha}s}{Is^2 + b_{\alpha}s + k_{\alpha}} A_d(s) + \frac{l}{Is^2 + b_{\alpha}s + k_{\alpha}} F_x(s) + \frac{l}{Is^2 + b_{\alpha}s + k_{\alpha}} D_{\alpha} \quad (\text{B.13})$$

Since  $l$ ,  $b_{\alpha}$  and  $k_{\alpha}$  are all strictly positive, the result shows that the control law for  $\alpha$  is locally stable. Considering the double support phase where we can apply the virtual damper in the horizontal direction, since the desired horizontal velocity is constant,  $F_x \rightarrow 0$  after any transient motion. This means that  $\alpha$  will approach  $\alpha_d = 0$ . Even for the single support phase, we can choose a large value for  $k_{\alpha}$  to reject the disturbance due to  $F_x$  and  $d_{\alpha}$  which we assume to be bounded.

Note that, although the stability analysis done here assumes that the biped has massless legs, this does not mean that the VMC cannot be applied to a biped which has significant leg masses compared to the body.

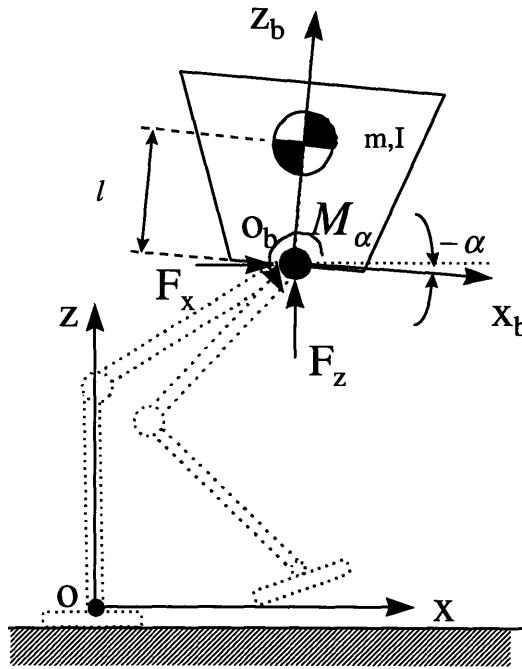


Figure B.1. Massless leg model for the biped

## References

---

- [Asada, 1986] H. Asada and J. E. Slotine, *Robot Analysis and Control*, Wiley, 1986.
- [Furusho and Masubuchi, 1986] J. Furusho and M. Masubuchi, "Control of a Dynamical Biped Locomotion System for Steady Walking," *Journal of Dynamical Systems, Measurement, and Control*, Vol. 108, pp 111-118, June 1986.
- [Kajita and Tani, 1996] S. Kajita and K. Tani, "Adaptive Gait Control of a Biped Robot based on Realtime Sensing of the Ground Profile," *Proc. Of IEEE International Conference on Robotics and Automation*, pp 570-577, April 1996.
- [Kajita and Tani, 1995] S. Kajita and K. Tani, "Experimental Study of Biped Dynamic Walking," *Proc. of IEEE International Conference on Robotics and Automation*, May 1995.
- [Kajita and Tani, 1991] S. Kajita and K. Tani, "Study of Dynamic Biped Locomotion on Rugged Terrain: Derivation and Application of the Linear Inverted Pendulum Mode," *Proceedings of the 1991 IEEE International Conf. on Robotics and Automation*, California, pp 1405-1411, April 1991.
- [McGeer, 1990] T. McGeer, "Passive Dynamic Walking," *International Journal of Robotics Research*, vol. 9, no. 2, pp 62-82, 1990.
- [Mitobe, et al., 1995] K. Mitobe, N. Mori, K. Aida and Y. Nasu, "Nonlinear Feedback Control of a Biped Walking Robot," *Proc. of IEEE International Conference on Robotics and Automation*, pp 2865-2870, 1995.
- [Muybridge, 1989] E. Muybridge, *The Human Figure in Motion*. Published by Dover Pubns, 1989.
- [Pratt, 1995] J. E. Pratt, "Virtual Model Control of a Biped Walking Robot," Master Thesis for Department of Engineering in Electrical Engineering and Computer Science, MIT, August 1995.
- [Pratt and Williamson, 1995] G. A. Pratt and M. M. Williamson, "Series Elastic Actuators," *Proc. of IEEE International Conference on Intelligent Robots and Systems*, pp 399-406, 1995.
- [Raibert, 1986] M. H. Raibert, *Legged Robots That Balance*. Cambridge, MA: MIT Press, 1986.
- [Raibert, 1986a] M. H. Raibert, "Legged Robots," *Communications of the ACM*, vol.29, no.6, June 1986.
- [Raibert, 1990] M. H. Raibert, "Legged Robots," *Artificial Intelligence at MIT Expanding Frontiers*, Edited by P. H. Winston, MIT Press, vol. 2, pp 149-179, 1990.
- [Slotine and Coetsee, 1986] J.-J. E. Slotine and J. A. Coetsee, "Adaptive sliding controller synthesis for non-linear systems," *Int. J. Control*, vol. 43, no. 6, pp 1631-1651, 1986.
- [Slotine and Li, 1991] J. E. Slotine and W. P. Li, *Applied Nonlinear Control*, Prentice Hall, 1991.
- [Song and Waldron, 1989] S. M. Song and K. J. Waldron, *Machines That Walk*, MIT Press, 1989.
- [Tzafestas et al., 1996] S. Tzafestas, M. Raibert and C. Tzafestas, "Robust Sliding-mode Control Applied to a 5-link Biped Robot," *Journal of Intelligent and Robotics Systems*, 15, pp 67-133, 1996.
- [Yamaguchi, et al., 1996] J. Yamaguchi, N. Kinoshita, A. Takanishi and I. Kato, "Development of a Dynamic Biped Walking System for Humanoid: Development of a Biped Walking Robot Adapting to the Humans' Living Floor," *Proc. of IEEE International conference on Robotics and Automation*, pp 232-239, 1996.
- [Yang, 1994] J. S. Yang, "A Control Study of a Kneeless Biped Locomotion System," *Journal of the Franklin Institute*, vol. 331B, no. 2, pp 125-143, 1994.
- [Zheng and Shen, 1990] Y. F. Zheng and J. Shen, "Gait Synthesis for the SD-2 Biped Robot to Sloping Surface," *IEEE Transactions on Robotics and Automation*, vol. 6, no. 1, pp 86-96, Feb 1990.